

0.2

NACA

RESEARCH MEMORANDUM

INVESTIGATION OF AERODYNAMIC CHARACTERISTICS IN PITCH
AND SIDESLIP OF A 45° SWEEPBACK-WING AIRPLANE MODEL
WITH VARIOUS VERTICAL LOCATIONS OF WING AND
HORIZONTAL TAIL

*6 Affinity
Date 3-10-59*

STATIC LONGITUDINAL STABILITY AND CONTROL, $M = 2.01$

By M. Leroy Spearman and Cornelius Driver

Langley Aeronautical Laboratory
Langley Field, Va.

*By Authority of NACA PA 4
WB 3-19-59*

CLASSIFIED DOCUMENT

This material contains information affecting the National Defense of the United States within the meaning of the espionage laws, Title 18, U.S.C., Secs. 793 and 794, the transmission or revelation of which in any manner to an unauthorized person is prohibited by law.

**NATIONAL ADVISORY COMMITTEE
FOR AERONAUTICS**

WASHINGTON

February 21, 1956

CONFIDENTIAL

UNCLASSIFIED

UNCLASSIFIED

To

By



NATIONAL ADVISORY COMMITTEE FOR AERONAUTICS

RESEARCH MEMORANDUM

INVESTIGATION OF AERODYNAMIC CHARACTERISTICS IN PITCH
AND SIDESLIP OF A 45° SWEEPBACK-WING AIRPLANE MODEL
WITH VARIOUS VERTICAL LOCATIONS OF WING AND
HORIZONTAL TAIL

STATIC LONGITUDINAL STABILITY AND CONTROL, $M = 2.01$

By M. Leroy Spearman and Cornelius Driver

SUMMARY

An investigation has been conducted in the Langley 4- by 4-foot supersonic pressure tunnel to determine the effects of various vertical locations of the wing and horizontal tail on the aerodynamic characteristics in pitch of a supersonic airplane configuration at a Mach number of 2.01. The model was equipped with a wing and horizontal tail, each having a 45° sweep and an aspect ratio of 4. The wing had a taper ratio of 0.2 with NACA 65A004 airfoil sections, whereas the horizontal tail had a taper ratio of 0.6 with NACA 65A006 airfoil sections.

The configurations investigated included a high-wing, a mid-wing, and a low-wing arrangement, each with four different horizontal tail locations varying from a position 0.208 semispan below to 0.556 semispan above the body center line. Tests were made with the horizontal tail both on and off and with the wing both on and off.

The results indicate significant changes in pitching moment at constant lift for the various horizontal-tail positions. The mid-high tail position provided the most positive increment in pitching moment with an attendant increase in the trim lift coefficients.

INTRODUCTION

The experimentally determined effects of wing and tail position on the aerodynamic characteristics of generalized aircraft configurations can be of considerable usefulness to the designer in the estimation of the stability and performance of similar specific configurations. In addition, such generalized results may be useful in the verification of various calculative methods for the prediction of the aerodynamic characteristics of airplanes. A considerable amount of such experimental data is available at low speeds (refs. 1 to 5, for example), wherein the influence of both plan form and position of wings and tails has been determined from wind-tunnel tests of models simulating high-speed type aircraft. Similar investigations have been extended to high subsonic Mach numbers (for example, refs. 5 to 9) and some results concerning the effects of tail location on the longitudinal characteristics of some rocket-propelled models have been obtained through the transonic speed range (refs. 10 and 11). Only a limited amount of such experimental data is available at present in the supersonic speed range. One example is the investigation reported in reference 12 in which the effects of wing-vertical location on the longitudinal characteristics of wing-body combinations were determined in the Mach number range from 0.61 to 0.91 and from 1.20 to 1.90.

In order to provide additional results of general interest to the designer for the supersonic speed range, an investigation has been conducted in the Langley 4- by 4-foot supersonic pressure tunnel at a Mach number of 2.01 to determine the effects of wing-vertical location and horizontal tail-vertical location on the longitudinal and lateral aerodynamic characteristics of a complete model having a 45° swept wing and tail. The basic results, without analysis, are presented in reference 13. An analysis of the effects of wing location and geometric dihedral for the wing-body combination is presented in reference 14. This paper presents the static longitudinal stability and control characteristics at $M = 2.01$ for the high-wing, mid-wing, and low-wing configurations, each with four different vertical positions of the horizontal tail. In addition, results are presented for each tail position with the wing removed. Several tail incidence angles in the range from 3.2° to -5.8° were investigated.

SYMBOLS

The results are presented as standard NACA coefficients of forces and moments. The data are referred to the stability axis system (fig. 1) with the reference center of moments located at 25 percent of the wing mean geometric chord.

The symbols are defined as follows:

C_L	lift coefficient, $-Z/qS$
C_D	drag coefficient, $-X/qS$
C_m	pitching-moment coefficient, $M'/qS\bar{c}$
C_{m_0}	pitching-moment coefficient at zero lift
Z	force along Z-axis
X	force along X-axis
M'	moment about Y-axis
q	free-stream dynamic pressure
S	wing area including body intercept
b	wing span
\bar{c}	wing mean geometric chord
α	angle of attack, deg
i_t	horizontal-tail incidence angle, deg
ϵ	effective downwash angle, deg
L/D	lift-drag ratio, C_L/C_D
n_p	neutral-point location, percent \bar{c}

MODEL AND APPARATUS

A drawing of the model is shown in figure 2 and the geometric characteristics of the model are presented in table I.

The model fuselage was a body of revolution having a length-diameter ratio of about 11 and was composed of an ogive nose, a cylindrical mid-section, and a slightly boattail rear section. The wing had 45° of sweep at the quarter-chord line, aspect ratio 4, taper ratio 0.2, and NACA 65A004 sections in the stream direction. The horizontal tail had 45° of

sweep at the quarter-chord line, an aspect ratio of 4, a taper ratio of 0.6, and NACA 65A006 sections in the stream direction. The model was equipped with a vertical tail with a small ventral fin and employed relatively thick slab-type sections to facilitate mounting of the horizontal tail. The position of the horizontal tail was variable from a point below the body on the ventral fin ($0.208b/2$ below body center line - designated tail position 4) to three positions above the body on the vertical tail ($0.208b/2$, $0.382b/2$, and $0.556b/2$ above body center line - designated as tail positions 3, 2, and 1, respectively). The uppermost location (tail position 1) was atop the vertical tail corresponding to a T-tail arrangement. Provisions were made for manually varying the incidence angle of the horizontal tail. The model was so designed that the wing position could be varied from a position flush with the underside of the body to the body center line or to a position flush with the upper surface of the body. The high- and low-wing positions were achieved by merely inverting the same wing. The mid wing was composed of two separate panels. The dihedral angle and the incidence angle were zero for all wings.

Force measurements were made through the use of a six-component internal strain-gage balance. The angle-of-attack range extended from 0° to about 18° and the tail incidence angle was varied in the range from 3.2° to -5.8° .

TESTS, CORRECTIONS, AND ACCURACY

The conditions for the tests were:

Mach number	2.01
Stagnation temperature, $^\circ\text{F}$	110
Stagnation pressure, lb/sq in. abs	12
Reynolds number, based on \bar{c}	1.84×10^6

The stagnation dewpoint was maintained sufficiently low (-25°F or less) so that no condensation effects were encountered in the test section.

The sting angle was corrected for the deflection under load. The Mach number variation in the test section was approximately ± 0.01 and the flow-angle variation in the vertical and horizontal planes did not exceed about $\pm 0.1^\circ$. The base pressure was measured and the drag force was adjusted to a base pressure equal to the free-stream static pressure.

The estimated errors in the individual measured quantities are as follows:

C_L	± 0.008
C_D	± 0.002
C_m	± 0.0004
i_t , deg	± 0.2
α , deg	± 0.2

RESULTS

The results are presented in the following manner:

Aerodynamic characteristics in pitch, complete model:	Figure
High wing, tail 1	3(a)
High wing, tail 2	3(b)
High wing, tail 3	3(c)
High wing, tail 4	3(d)
Mid wing, tail 1	4(a)
Mid wing, tail 2	4(b)
Mid wing, tail 3	4(c)
Mid wing, tail 4	4(d)
Low wing, tail 1	5(a)
Low wing, tail 2	5(b)
Low wing, tail 3	5(c)
Low wing, tail 4	5(d)
Wing-off, tail 1	6(a)
Wing-off, tail 2	6(b)
Wing-off, tail 3	6(c)
Wing-off, tail 4	6(d)
Effect of wing position on longitudinal stability characteristics:	
Complete models	7(a)
Tail off	7(b)
Effect of tail position on longitudinal stability characteristics:	
Complete models	8
Wing off	9
Effect of wing and tail position on effective downwash:	
Angle	10
Effect of wing position on lift-drag ratio	11
Effect of tail position on lift-drag ratio	12
Summary of trim longitudinal characteristics	13

Although the data are presented without detailed analysis, a few remarks concerning the results might be made. Perhaps the most significant result is the variation with horizontal-tail position of C_m at a constant C_L or α (see figs. 8 and 9) since the magnitude of C_m dictates the amount of control deflection required for trim. In general, tail position 4 provides the lowest values of C_m while relatively large positive shifts in C_m are indicated for tail position 2. Similar variations are, of course, reflected in the effective downwash angles as well (fig. 10).

It is interesting to note that the C_{m_0} shifts and that the ϵ characteristics are essentially the same for each wing position as well as for the wing removed; thus, the possibility of any major influence of the wing flow field on these characteristics is small. The relative effects of the remaining possible influencing factors, such as the body-induced flow field and the vertical-tail-induced flow field, are somewhat obscure.

Some indication of the body flow-field effect can be obtained by comparing the effective downwash angles measured for tail position 3 with those determined both theoretically and experimentally for a similar configuration at Mach numbers of 1.40 and 1.59 (ref. 15). A comparison of these results indicates that the effective downwash angles for tail position 3 are about the magnitude to be expected from consideration of the body flow field. However, it might be further pointed out that the C_{m_0} increments and ϵ increments at $\alpha = 0^\circ$ provided by tails 3 and 4 (figs. 9 and 10) are not the same although these tails are located symmetrically with respect to the body flow field. In addition, tails 4 and 1, which are located quite differently with respect to the body flow field, indicate similar ϵ values and provide essentially zero increment in C_{m_0} . Hence, it is apparent that the C_{m_0} variations resulting from the various tail positions are influenced to some extent by the induced flows from the vertical tail acting on the horizontal tail. A similar conclusion was reached from tests of some configurations reported in reference 16.

The largest C_{m_0} increment was provided by tail 2 and the increments decrease successively for tails 3, 1, and 4. A similar trend in C_{m_0} variation with tail height for an unswept-wing model at $M = 1.92$ may be noted in reference 17 wherein the maximum C_{m_0} shift occurred for a tail height midway between a tail located on the body center line and one mounted near the tip of the vertical tail.

The significance of the more positive C_m values provided by tail 2 is apparent in the trim longitudinal characteristics of the configurations

(fig. 13). The higher trim lift coefficients indicated for tail position 2 would be reflected in improved altitude performance and maneuverability.

It might be pointed out that the maximum untrimmed value of L/D occurred for tail position 4 and was about 4.25 for all wing positions (fig. 11); whereas, the maximum trimmed values with $i_t = -5.8^\circ$ occurred for tail position 2 and varied from about 3.7 to 3.85.

CONCLUDING REMARKS

Results of an investigation conducted at a Mach number of 2.01 to determine the effects of various vertical locations of the wing and horizontal tail on the static longitudinal stability and control characteristics of a 45° swept-wing model indicated that significant variations in the pitching-moment coefficient at constant lift can be obtained through variations in the horizontal-tail vertical location. These variations in pitching-moment coefficient appear to be independent of the wing and are influenced primarily by the body-induced flows and the vertical-tail-induced flows.

The mid-high tail position provided the most positive increment in pitching moment with an attendant increase in the trim lift coefficients.

Langley Aeronautical Laboratory,
National Advisory Committee for Aeronautics,
Langley Field, Va., November 15, 1955.

REFERENCES

1. Goodman, Alex: Effects of Wing Position and Horizontal-Tail Position on the Static Stability Characteristics of Models With Unswept and 45° Sweptback Surfaces With Some Reference to Mutual Interference. NACA TN 2504, 1951.
2. Brewer, Jack D., and Lichtenstein, Jacob H.: Effect of Horizontal Tail on Low-Speed Static Lateral Stability Characteristics of a Model Having 45° Sweptback Wing and Tail Surfaces. NACA TN 2010, 1950.
3. Queijo, M. J., and Wolhart, Walter D.: Experimental Investigation of the Effect of Vertical-Tail Size and Length and of Fuselage Shape and Length on the Static Lateral Stability Characteristics of a Model With 45° Sweptback Wing and Tail Surfaces. NACA Rep. 1049, 1951. (Supersedes NACA TN 2168.)
4. Goodman, Alex, and Thomas, David F., Jr.: Effects of Wing Position and Fuselage Size on the Low-Speed Static and Rolling Stability Characteristics of a Delta-Wing Model. NACA TN 3063, 1954.
5. Wiggins, James W., Kuhn, Richard E., and Fournier, Paul G.: Wind-Tunnel Investigation To Determine the Horizontal- and Vertical-Tail Contributions to the Static Lateral Stability Characteristics of a Complete-Model Swept-Wing Configuration at High Subsonic Speeds. NACA RM L53E19, 1953.
6. Morrison, William D., Jr., and Alford, William J., Jr.: Effects of Horizontal-Tail Height and a Wing Leading-Edge Modification Consisting of a Full-Span Flap and a Partial-Span Chord-Extension on the Aerodynamic Characteristics in Pitch at High Subsonic Speeds of a Model With a 45° Sweptback Wing. NACA RM L53E06, 1953.
7. Alford, William J., Jr., and Pasteur, Thomas B., Jr.: The Effects of Changes in Aspect Ratio and Tail Height on the Longitudinal Stability Characteristics at High Subsonic Speeds of a Model With a Wing Having 32.6° Sweepback. NACA RM L53L09, 1954.
8. Goodson, Kenneth W., and Becht, Robert E.: Wind-Tunnel Investigation at High Subsonic Speeds of the Stability Characteristics of a Complete Model Having Sweptback-, M-, W-, and Cranked-Wing Plan Forms and Several Horizontal-Tail Locations. NACA RM L54C29, 1954.
9. Few, Albert G., Jr., and King, Thomas J., Jr.: Some Effects of Tail Height and Wing Plan Form on the Static Longitudinal Stability Characteristics of a Small-Scale Model at High Subsonic Speeds. NACA RM L54G12, 1954.

10. Parks, James H., and Kehlet, Alan B.: Longitudinal Stability, Trim, and Drag Characteristics of a Rocket-Propelled Model of an Airplane Configuration Having a 45° Sweptback Wing and an Unswept Horizontal Tail. NACA RM L52F05, 1952.
11. Parks, James H., and Kehlet, Alan B.: Longitudinal Stability and Trim of Two Rocket-Propelled Airplane Models Having 45° Sweptback Wings and Tails With the Horizontal Tail Mounted in Two Positions. NACA RM L53J12a, 1953.
12. Heitmeyer, John C.: Effect of Vertical Position of the Wing on the Aerodynamic Characteristics of Three Wing-Body Combinations. NACA RM A52L15a, 1953.
13. Spearman, M. Leroy, Driver, Cornelius, and Hughes, William C.: Investigation of Aerodynamic Characteristics in Pitch and Sideslip of a 45° Sweptback-Wing Airplane Model With Various Vertical Locations of Wing and Horizontal Tail - Basic-Data Presentation, $M = 2.01$. NACA RM L54L06, 1955.
14. Spearman, M. Leroy: Investigation of Aerodynamic Characteristics in Pitch and Sideslip of a 45° Sweptback-Wing Airplane Model With Various Vertical Locations of the Wing and Horizontal Tail - Effect of Wing Location and Geometric Dihedral for the Wing-Body Combination, $M = 2.01$. NACA RM L55B18, 1955.
15. Grant, Frederick C., and Gopcynski, John P.: An Investigation of a Supersonic Aircraft Configuration Having a Tapered Wing With Circular-Arc Sections and 40° Sweepback. Estimated Downwash Angles Derived From Pressure Measurements on the Tail at Mach Numbers of 1.40 and 1.59. NACA RM L51L17, 1952.
16. Smith, Willard G.: Wind-Tunnel Investigation at Subsonic and Supersonic Speeds of a Fighter Model Employing a Low-Aspect-Ratio Unswept Wing and a Horizontal Tail Mounted Well Above the Wing Plane - Longitudinal Stability and Control. NACA RM A54D05, 1954.
17. Ellis, Macon C., Jr., and Grigsby, Carl E.: Aerodynamic Investigation at Mach Number 1.92 of a Rectangular Wing and Tail and Body Configuration and Its Components. NACA RM L9L28a, 1950.

TABLE I.- GEOMETRIC CHARACTERISTICS OF MODEL

Wing:

Area, sq in.	144
Span, in.	24
Root chord, in.	10
Tip chord, in.	2
Taper ratio	0.2
Aspect ratio	4
Mean geometric chord, in.	6.89
Spanwise location of MGC, percent wing semispan	38.9
Incidence, deg	0
Sweep of quarter-chord line, deg	45
Airfoil section	NACA 65A004

Horizontal tail:

Area, sq in.	28.6
Span, in.	10.73
Root chord, in.	3.35
Tip chord, in.	2.01
Taper ratio	0.6
Aspect ratio	4
Sweep of quarter-chord line, deg	45
Airfoil section	NACA 65A006

Vertical tail (excluding ventral fin):

Area to body center line, sq in.	43.5
Span from body center line, in.	7.48
Root chord, in.	8.17
Tip chord, in.	3.44
Taper ratio	0.42
Aspect ratio	1.29
Sweep of leading edge, deg	35
Airfoil section	Wedge nose, slab side with constant thickness of 0.437 inch

Ventral fin:

Exposed area, sq in.	8.54
------------------------------	------

Body:

Length, in.	36.50
Diameter (maximum), in.	3.33
Diameter (base), in.	2.67
Length-diameter ratio	10.96

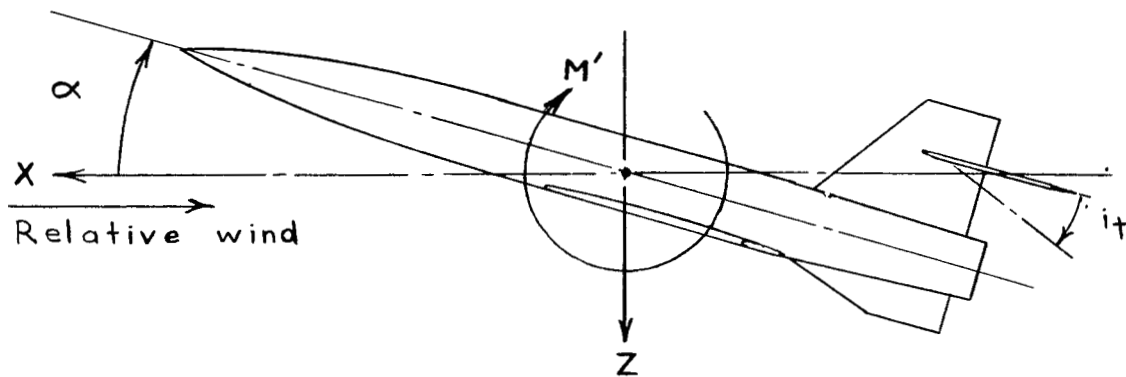


Figure 1.- System of stability axes. Arrows indicate positive directions.

	A	Λ	λ	Section
Wing	4	45°	.2	NACA 65A004
Stabilizer	4	45°	.6	NACA 65A006

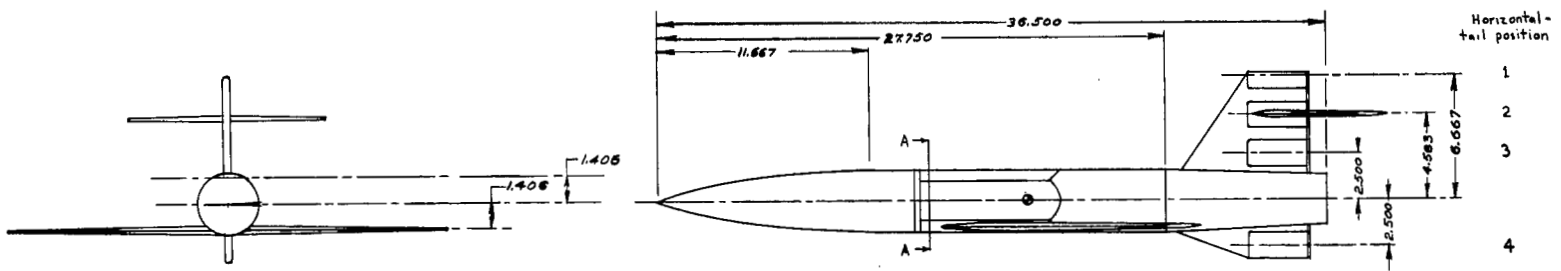
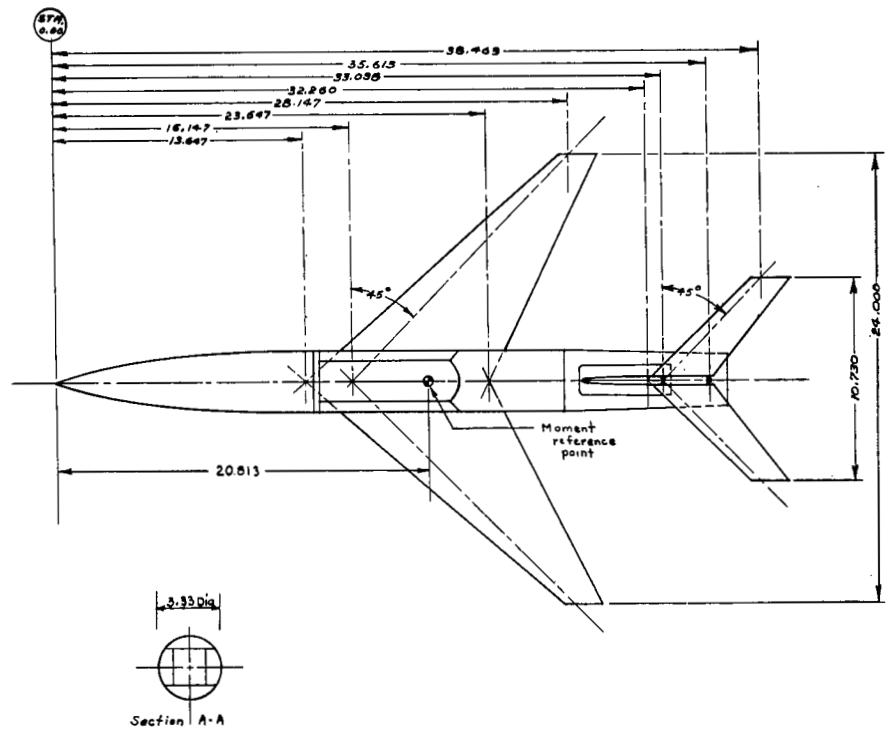
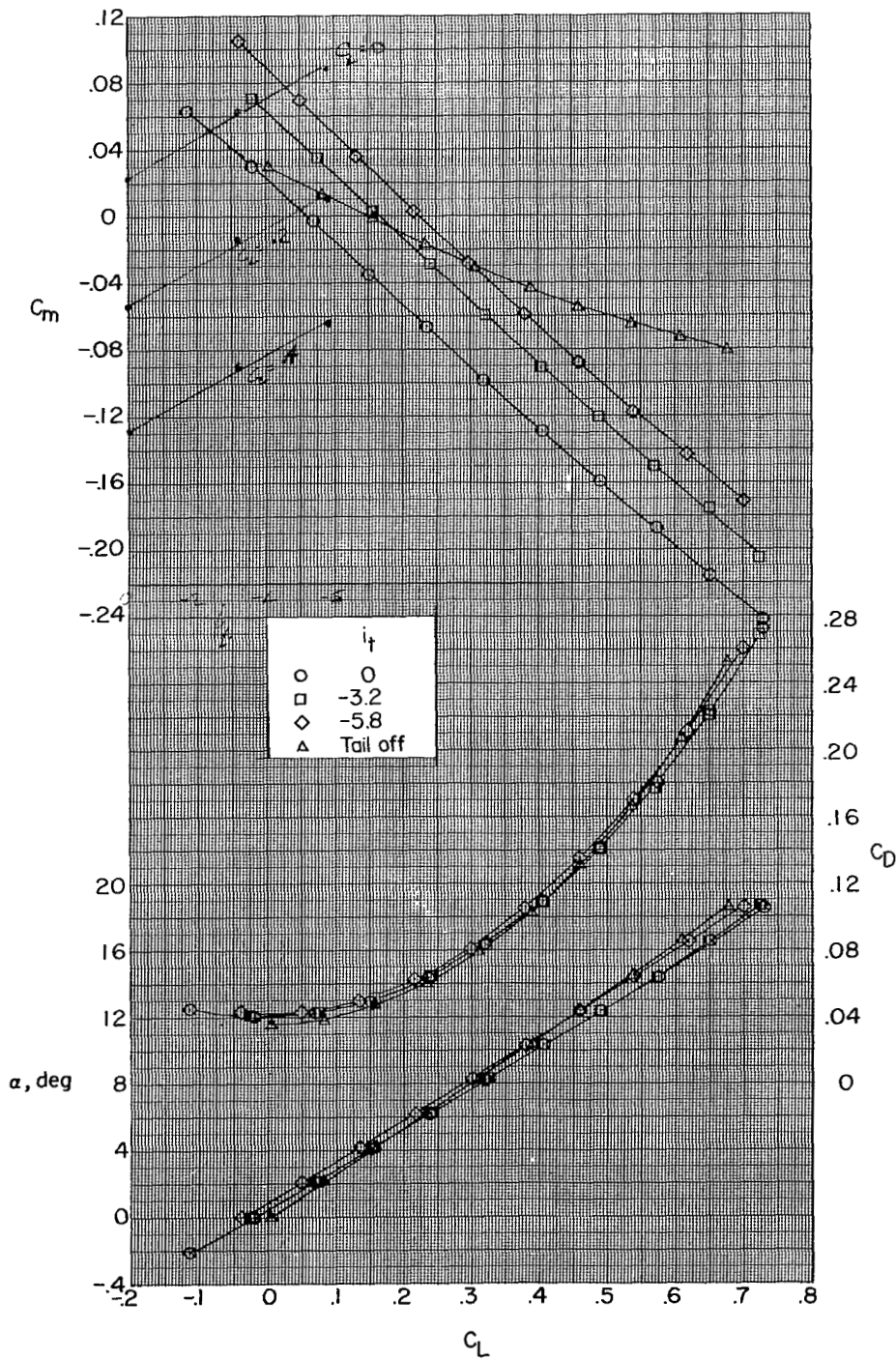
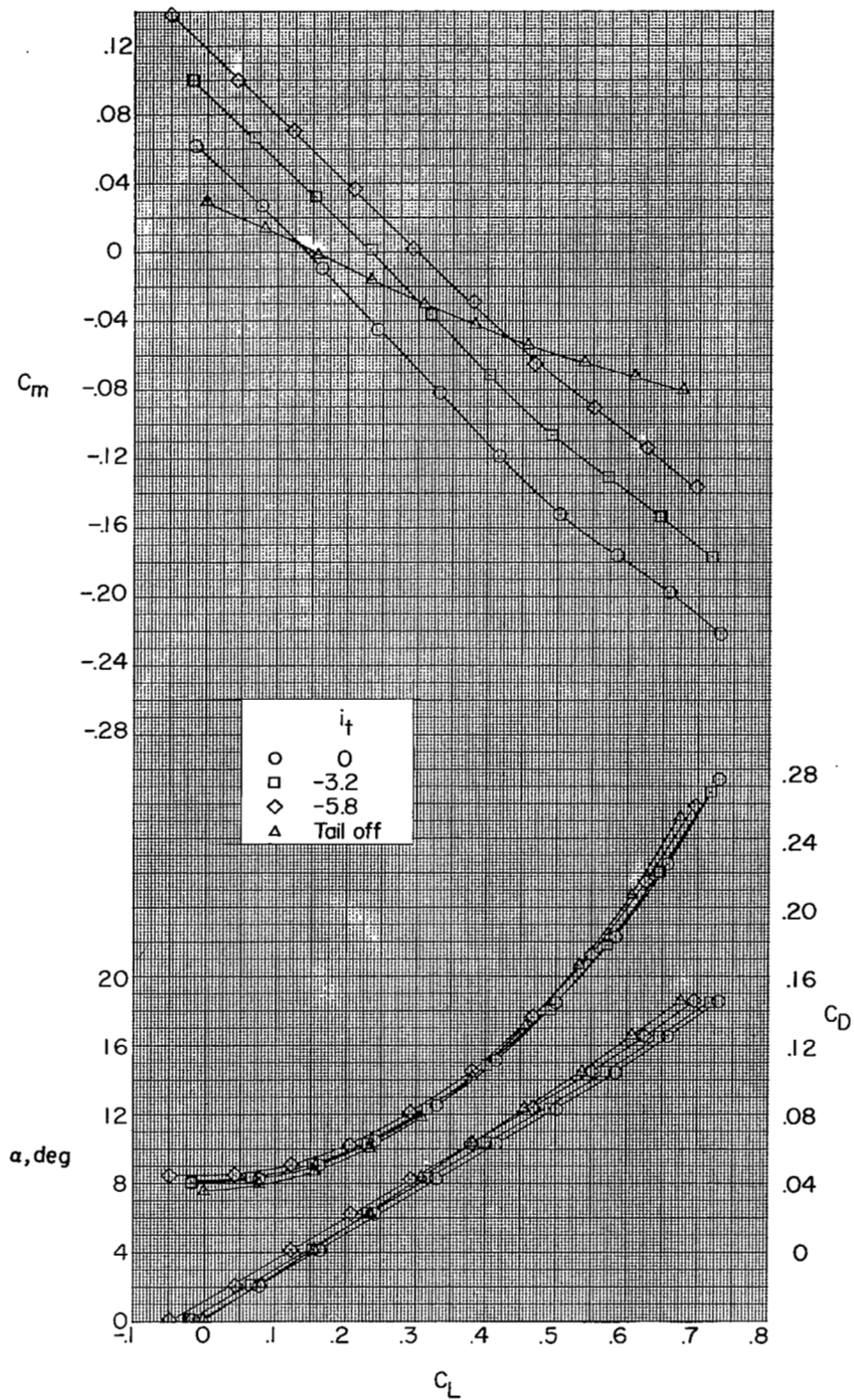


Figure 2.- Three-view drawing of model. All dimensions are in inches.



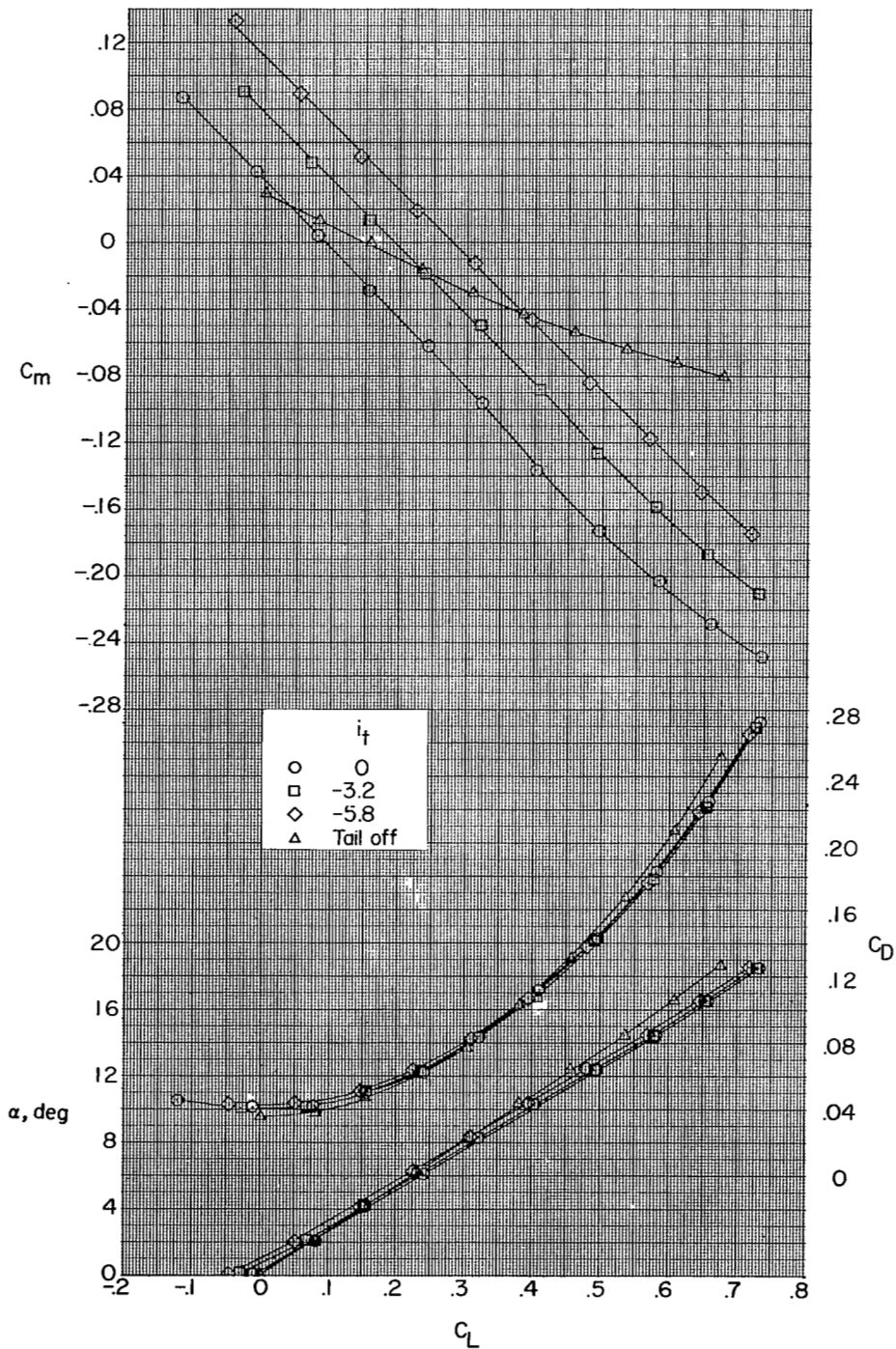
(a) Tail 1.

Figure 3.- Aerodynamic characteristics in pitch for high-wing configuration with various horizontal-tail locations.



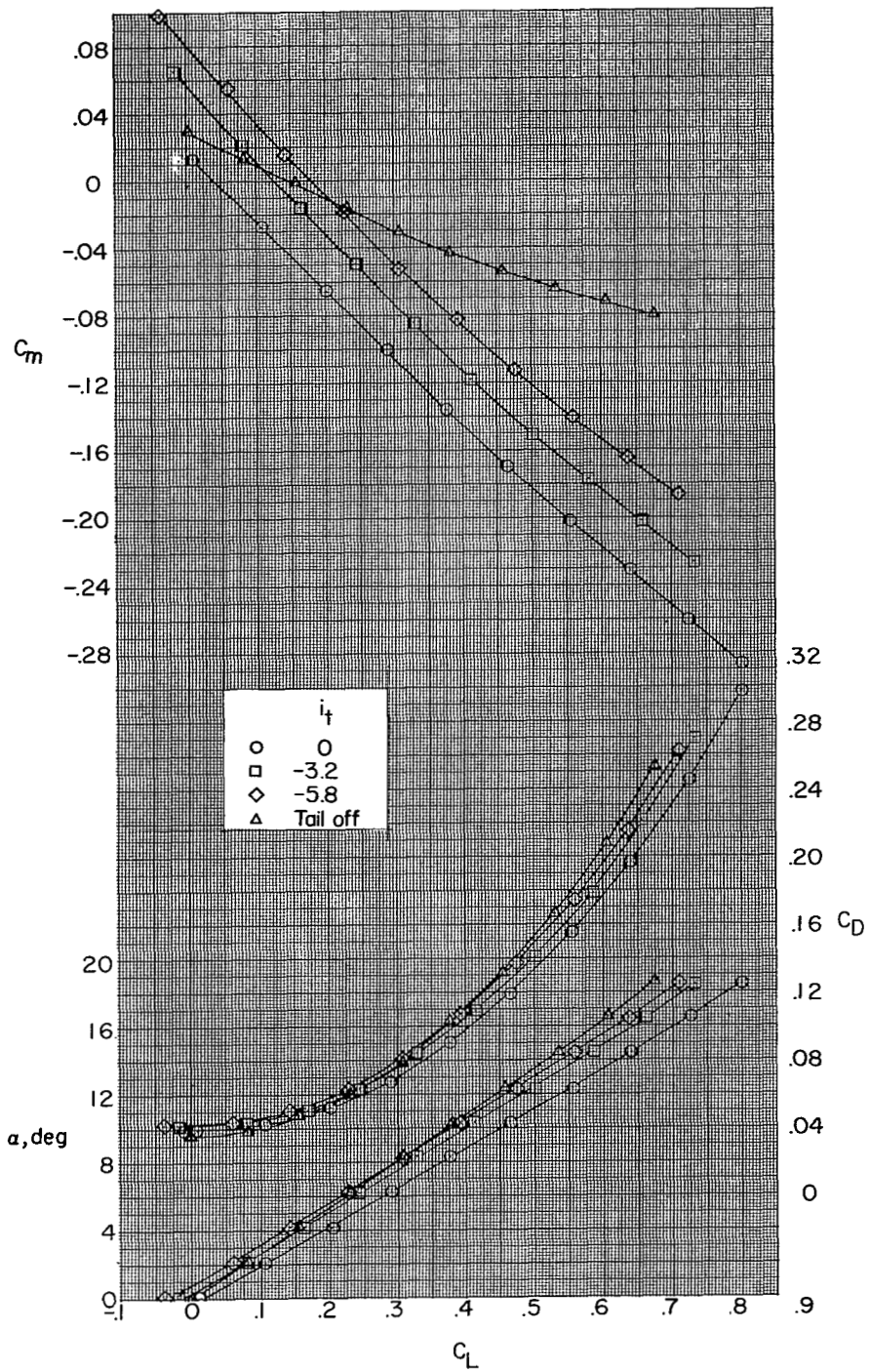
(b) Tail 2.

Figure 3.- Continued.



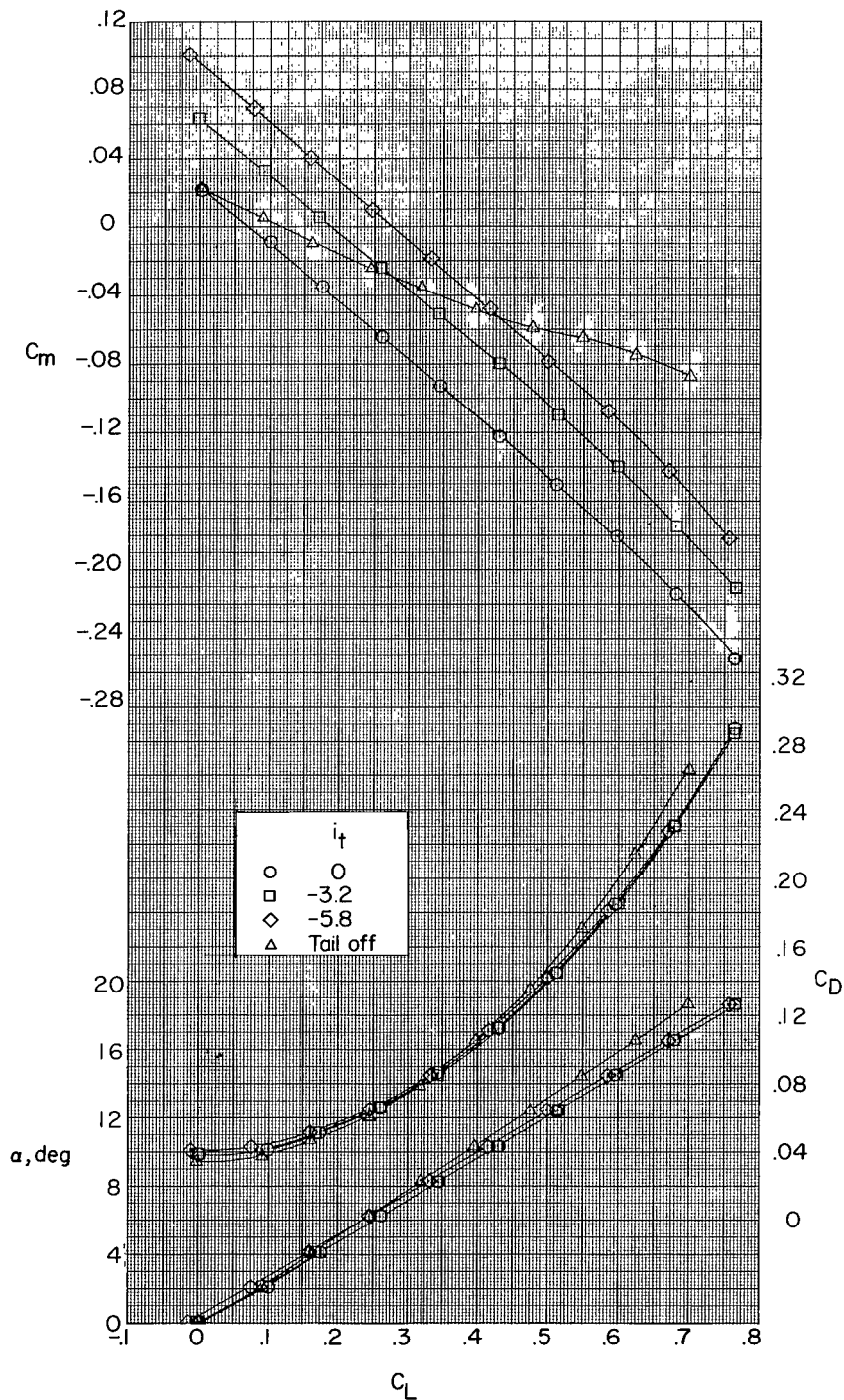
(c) Tail 3.

Figure 3.- Continued.



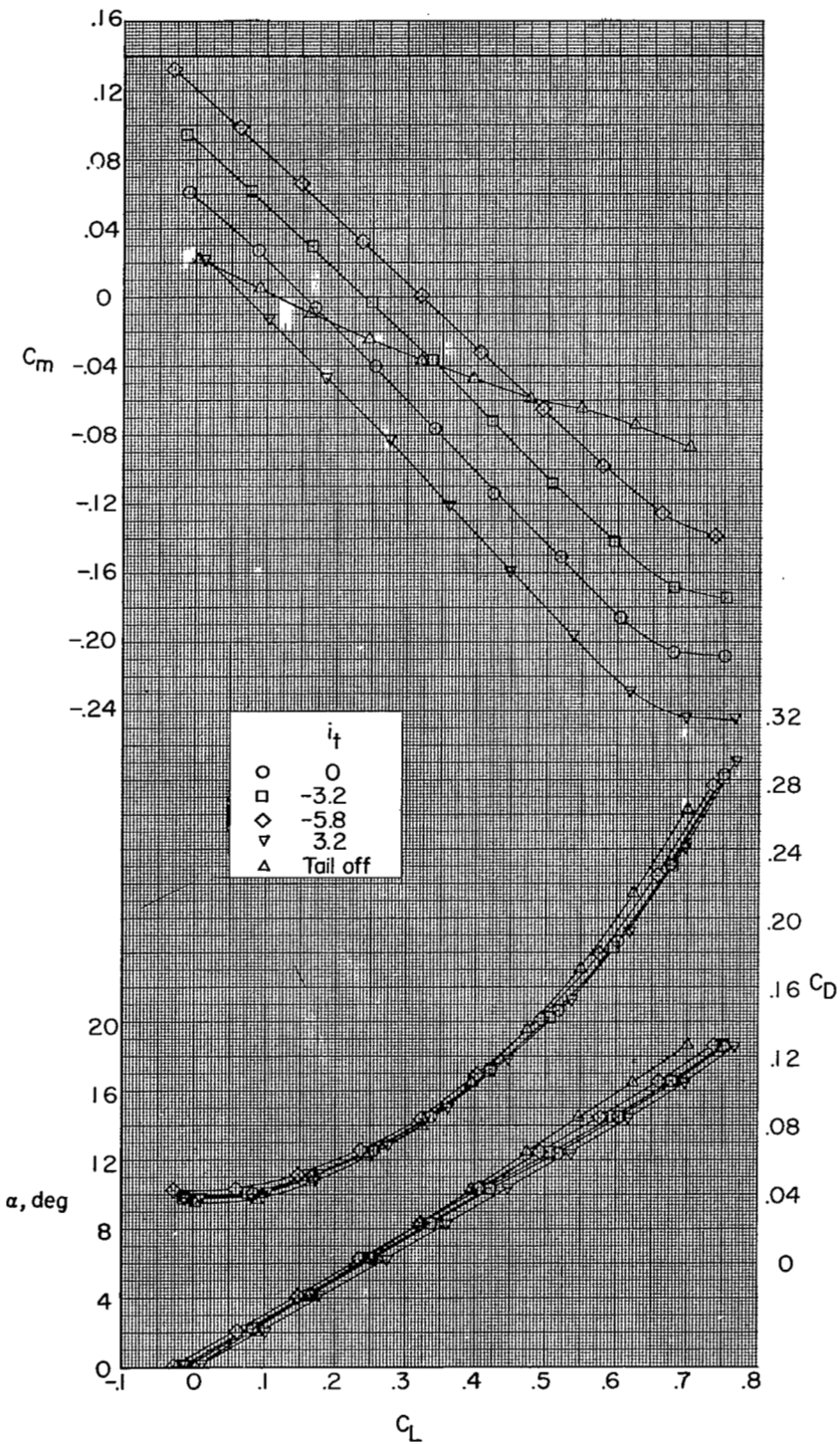
(d) Tail 4.

Figure 3.- Concluded.



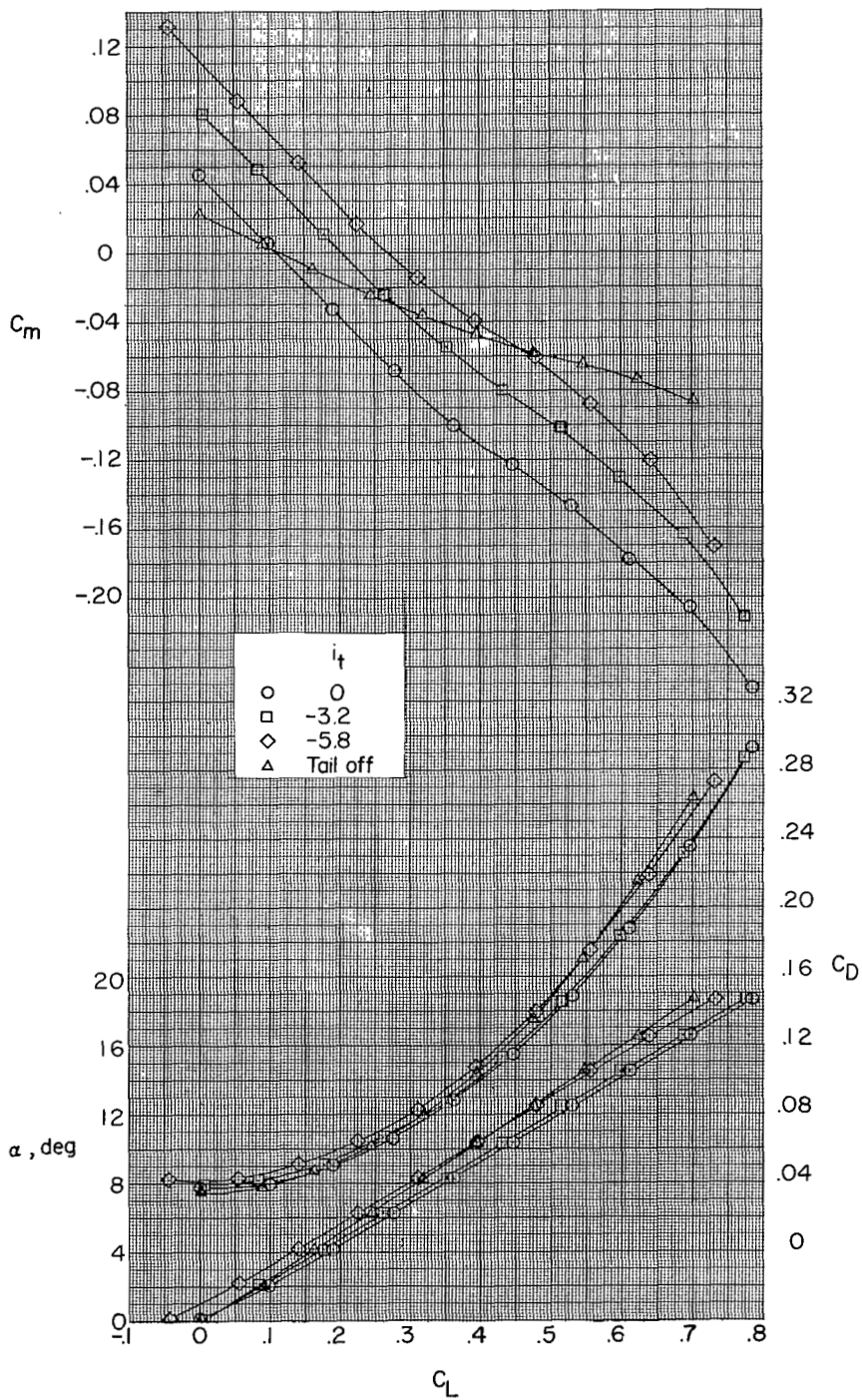
(a) Tail 1.

Figure 4.- Aerodynamic characteristics in pitch for mid-wing configuration with various horizontal-tail locations.



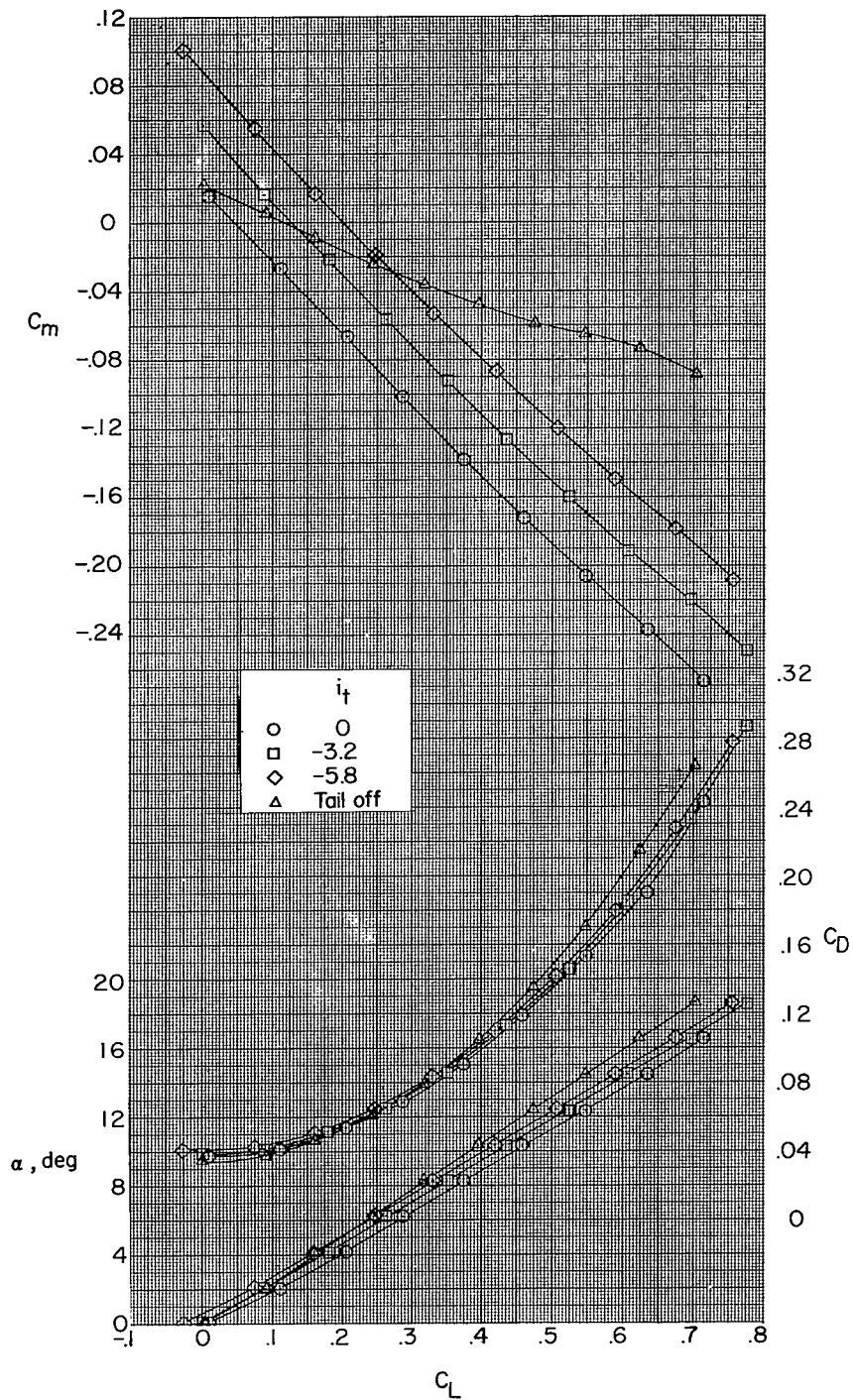
(b) Tail 2.

Figure 4.- Continued.



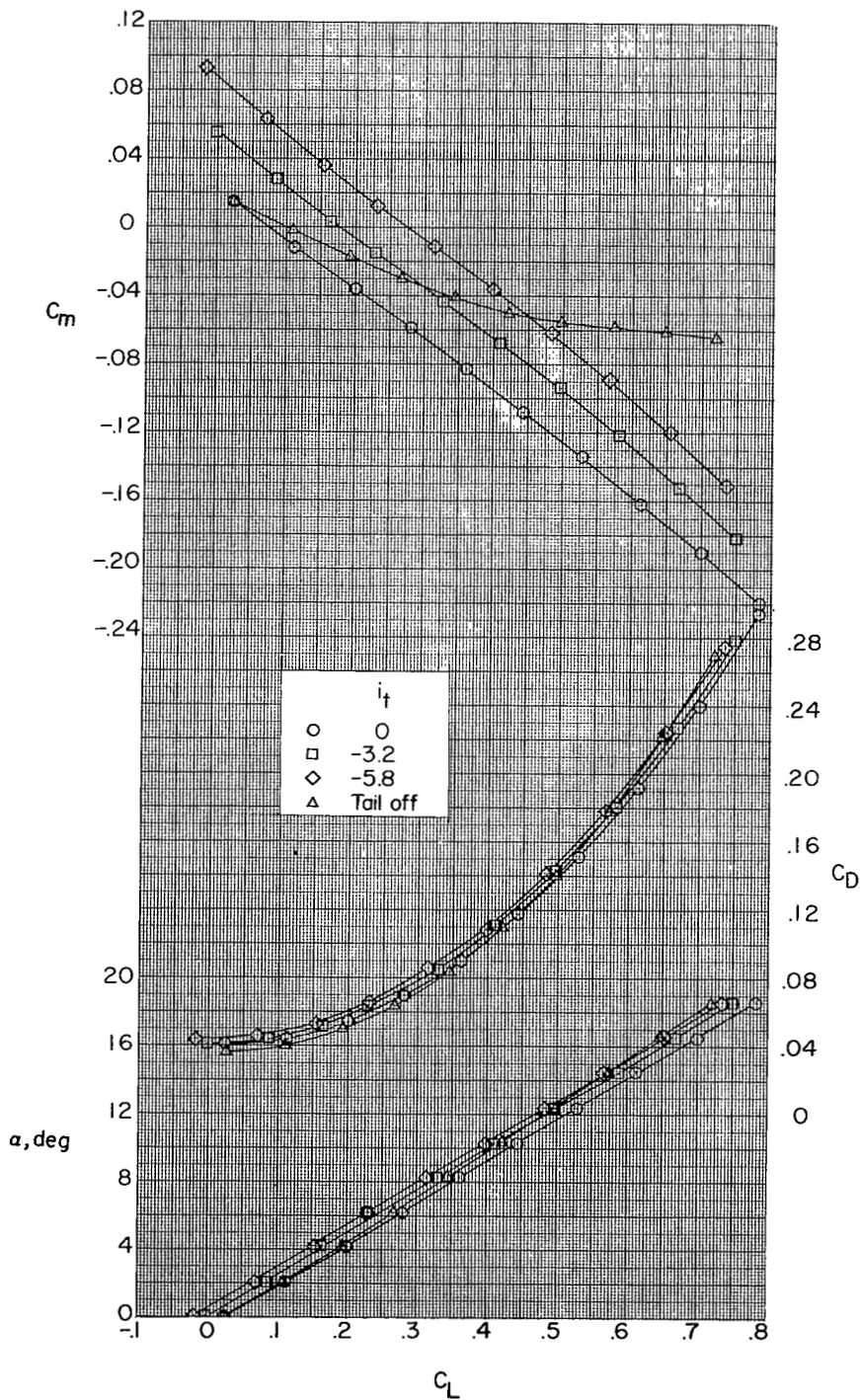
(c) Tail 3.

Figure 4.- Continued.



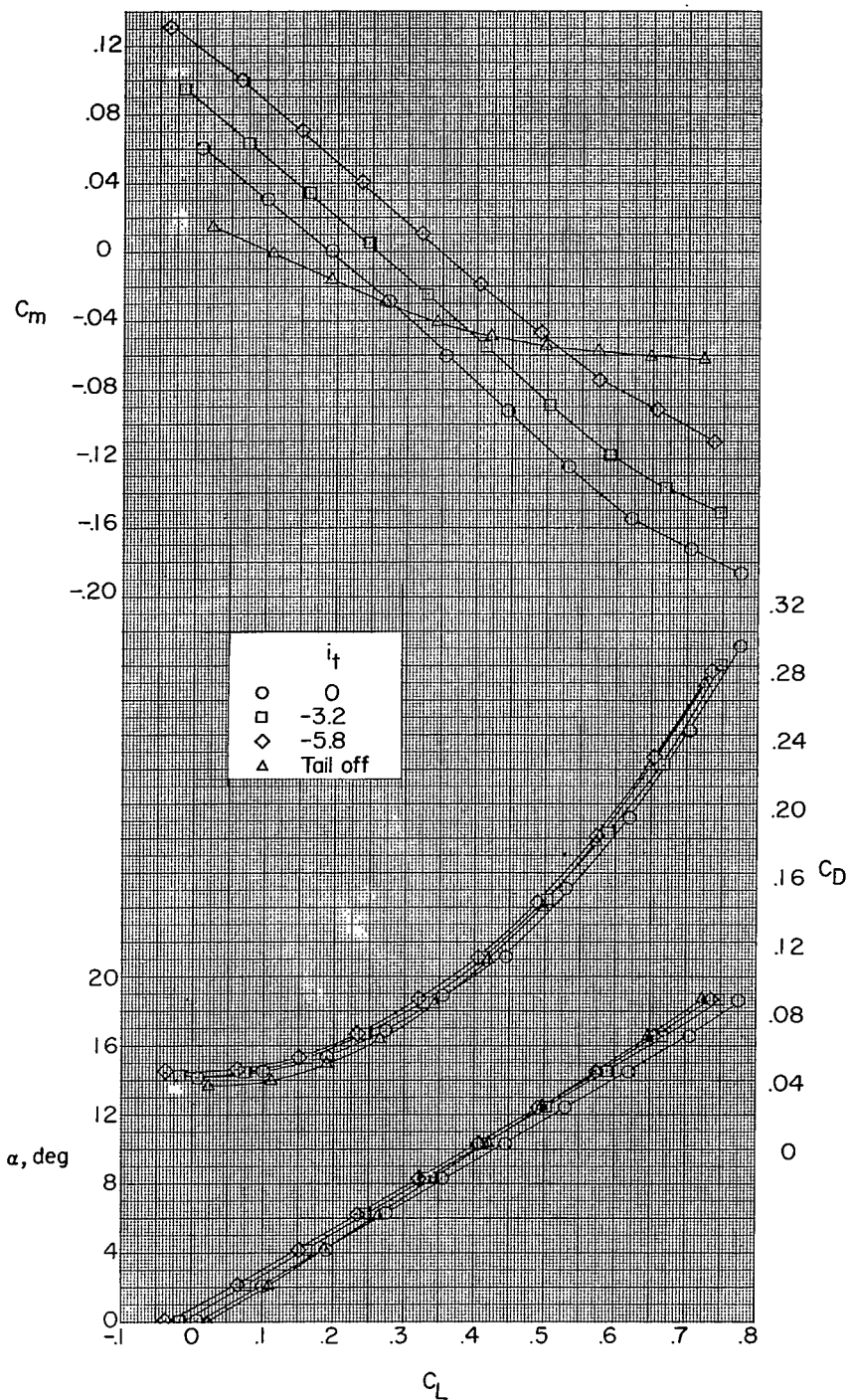
(d) Tail 4.

Figure 4.- Concluded.



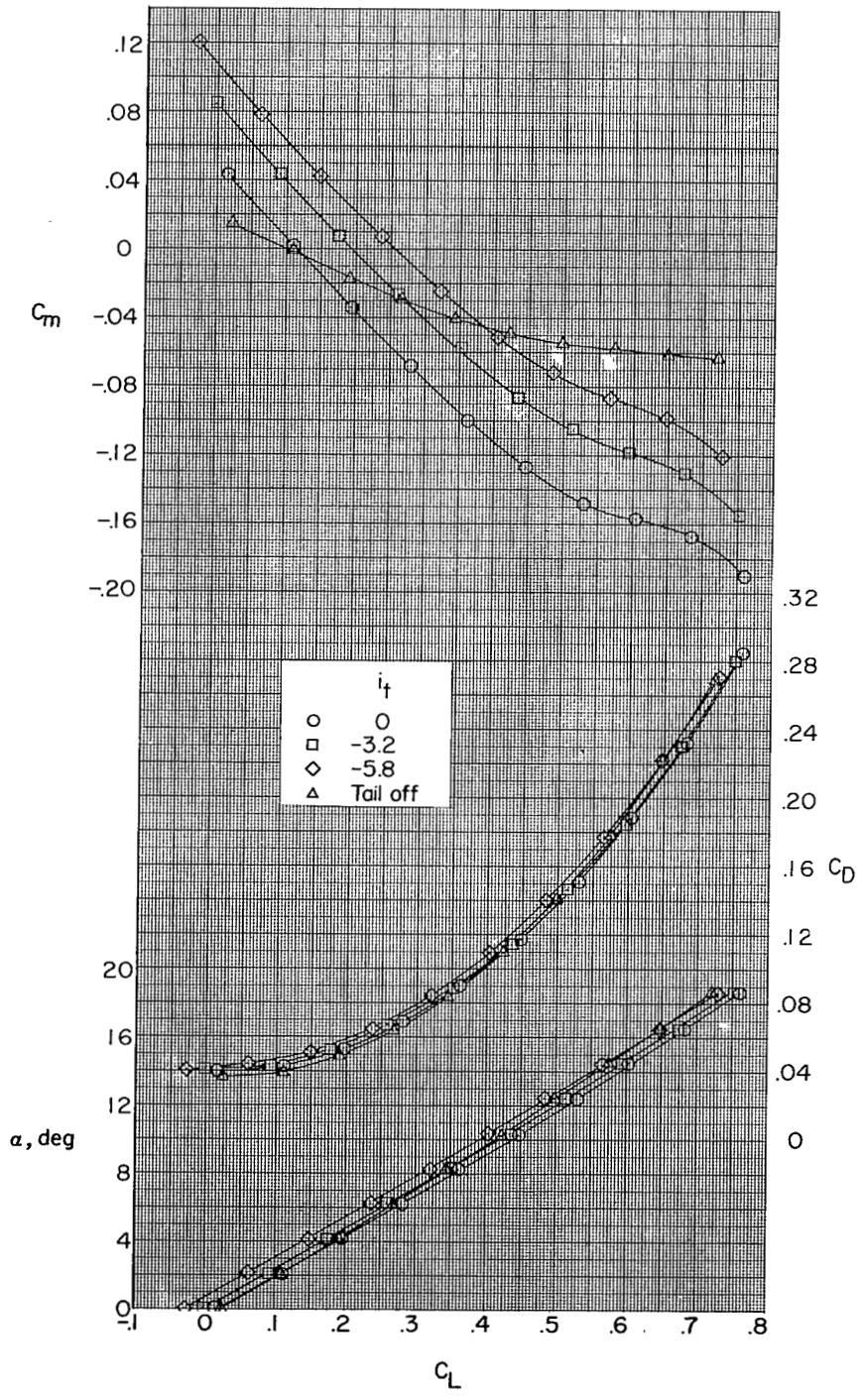
(a) Tail 1.

Figure 5.- Aerodynamic characteristics in pitch for low-wing configuration with various horizontal-tail locations.



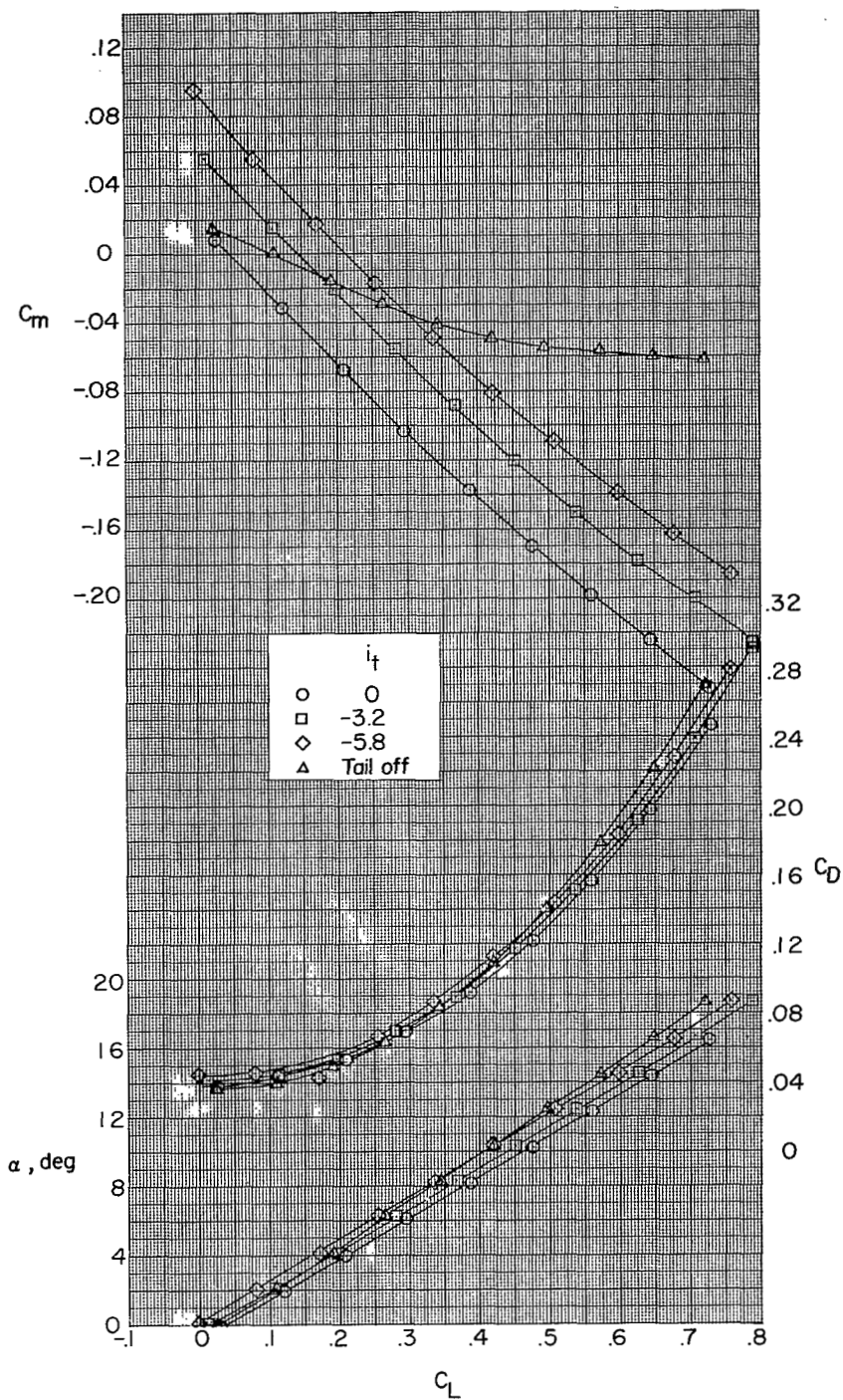
(b) Tail 2.

Figure 5.- Continued.



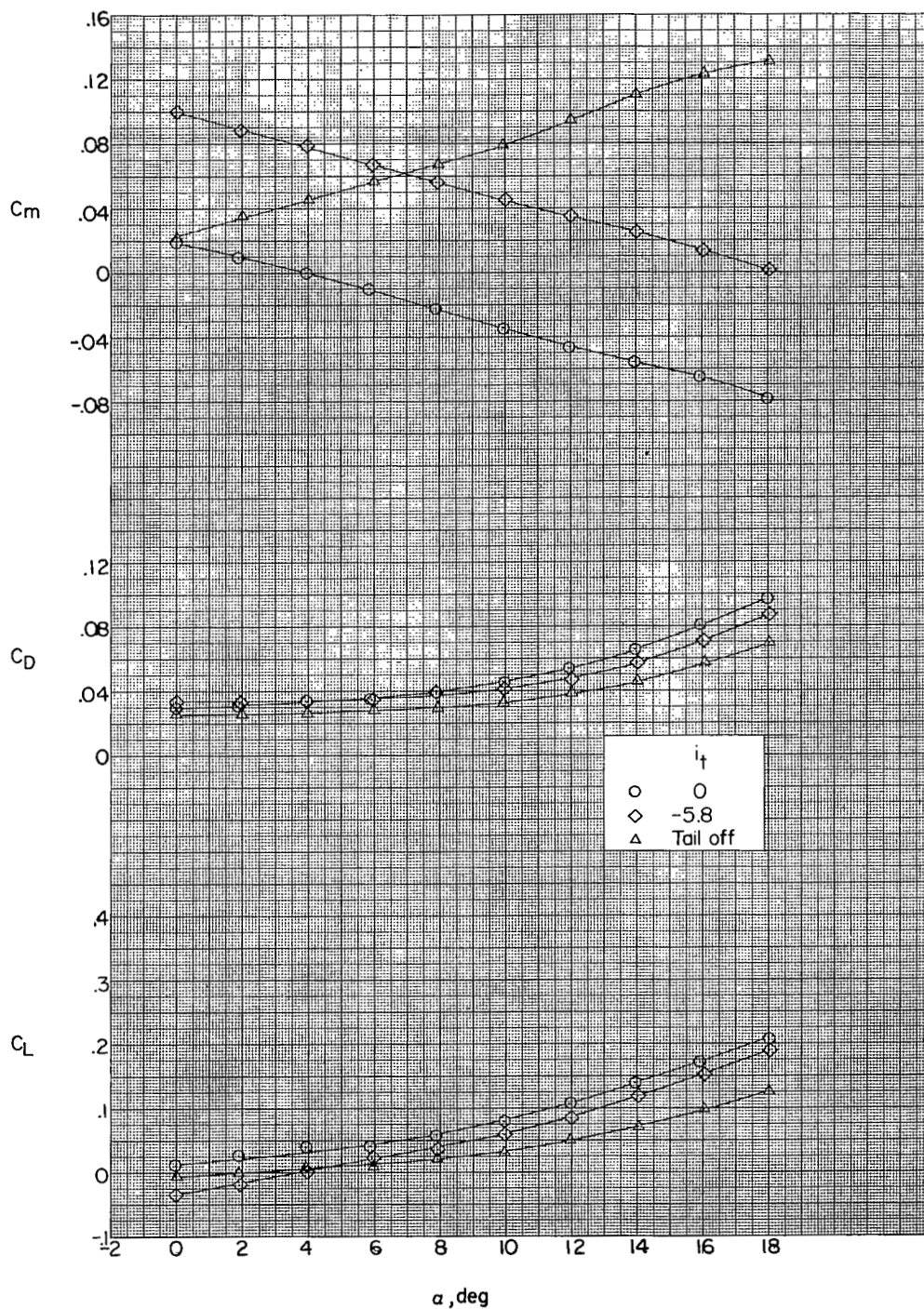
(c) Tail 3.

Figure 5.- Continued.



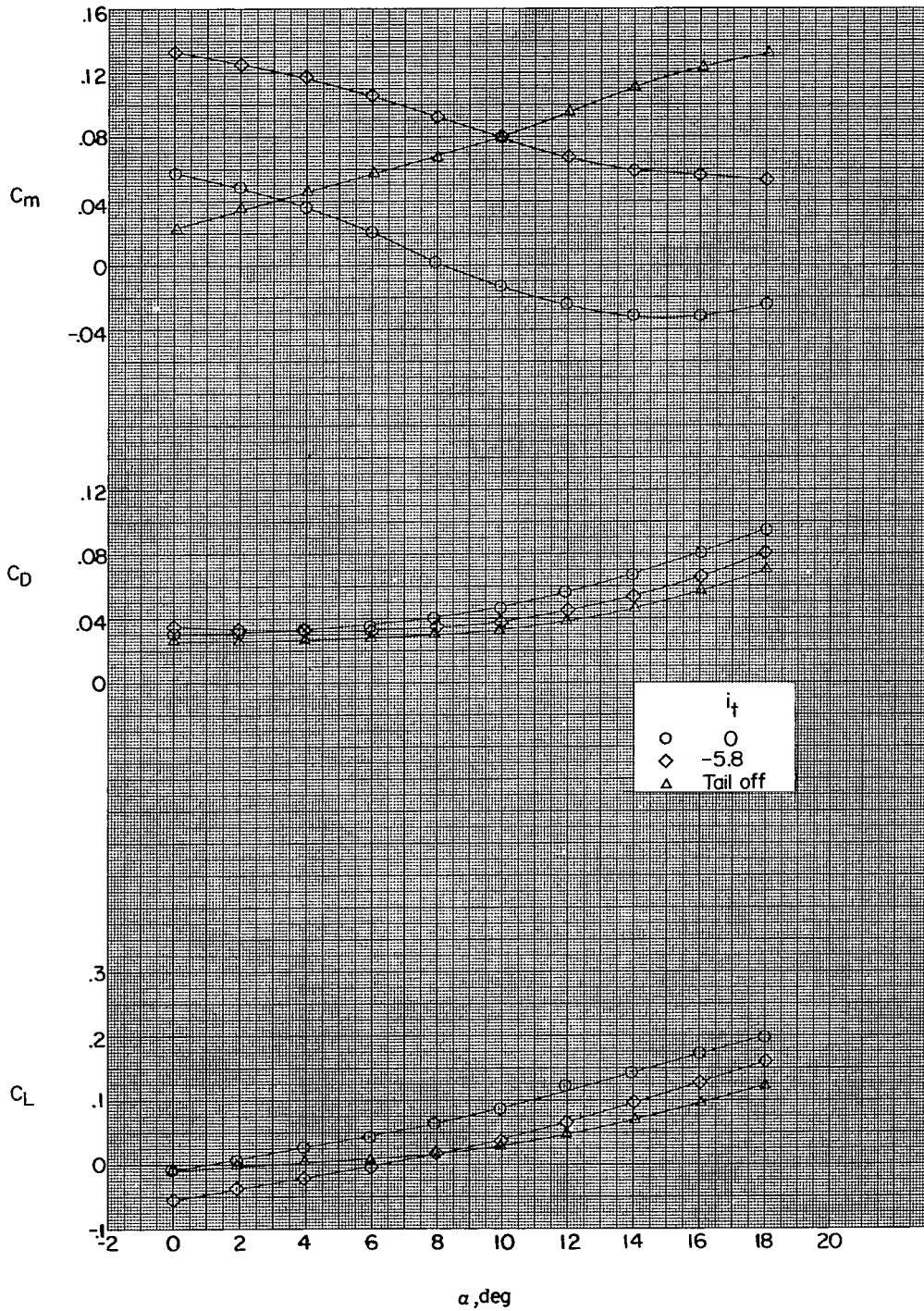
(d) Tail 4.

Figure 5.- Concluded.



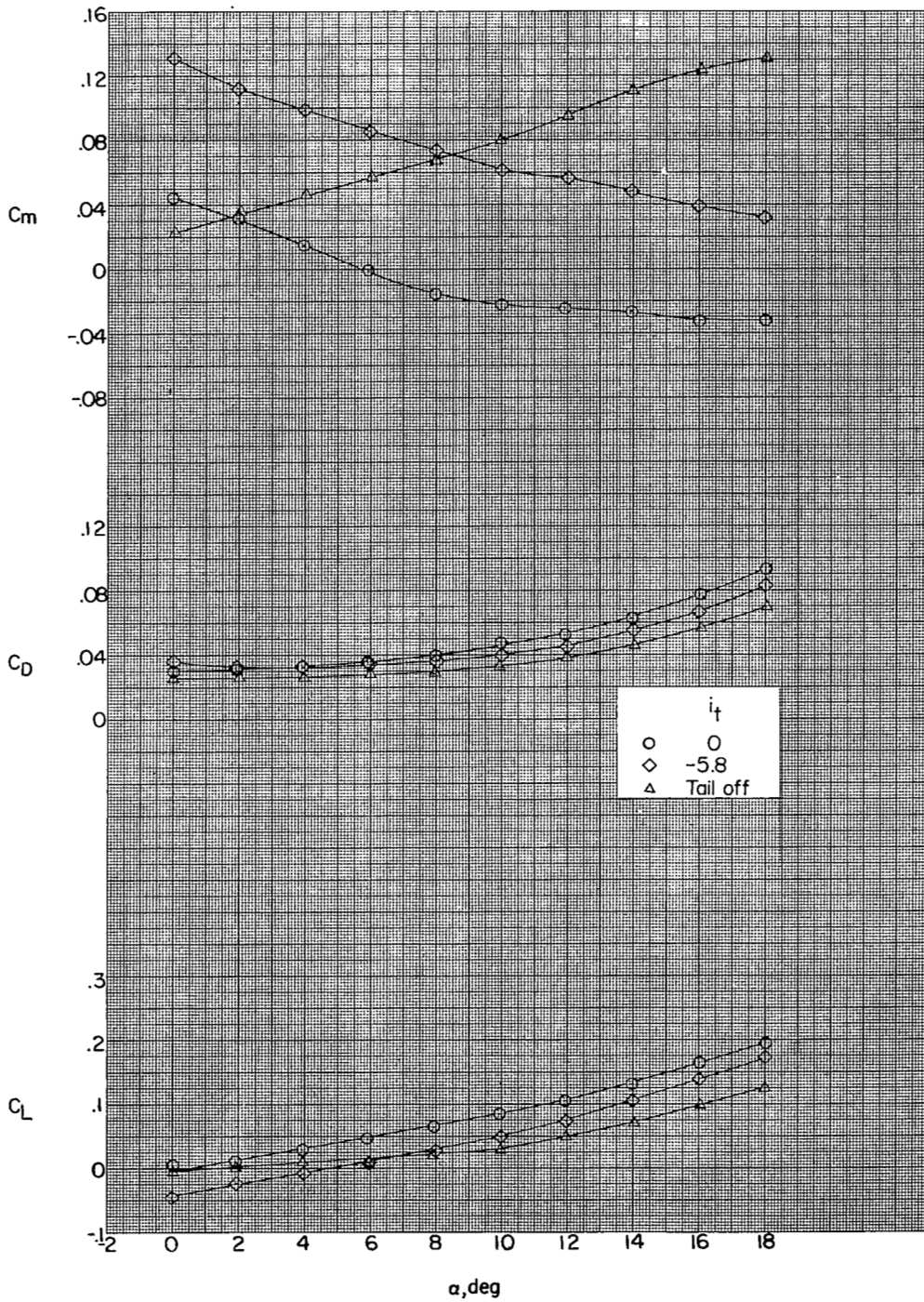
(a) Tail 1.

Figure 6.- Aerodynamic characteristics in pitch for wing-off configuration with various horizontal-tail locations.



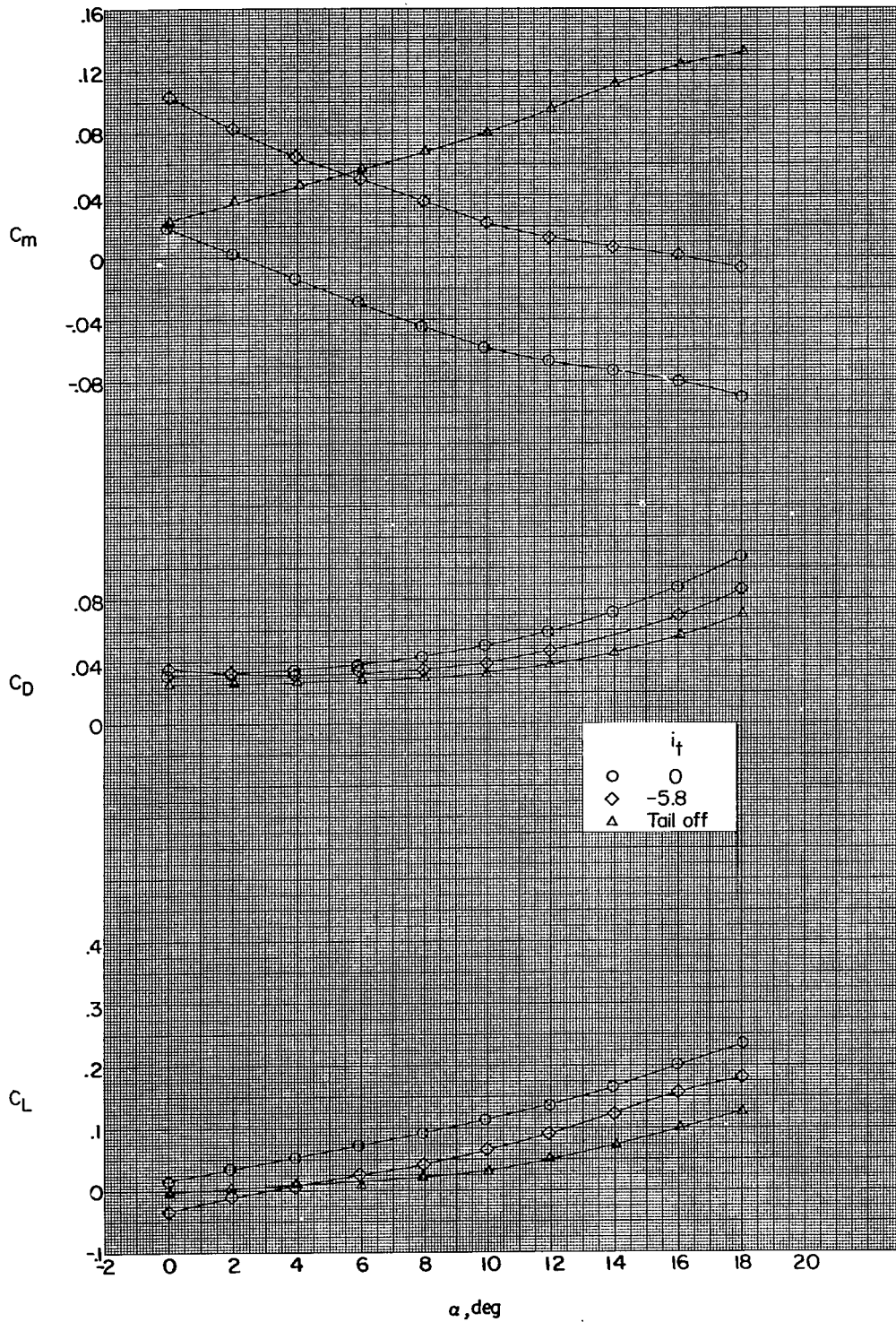
(b) Tail 2.

Figure 6.- Continued.



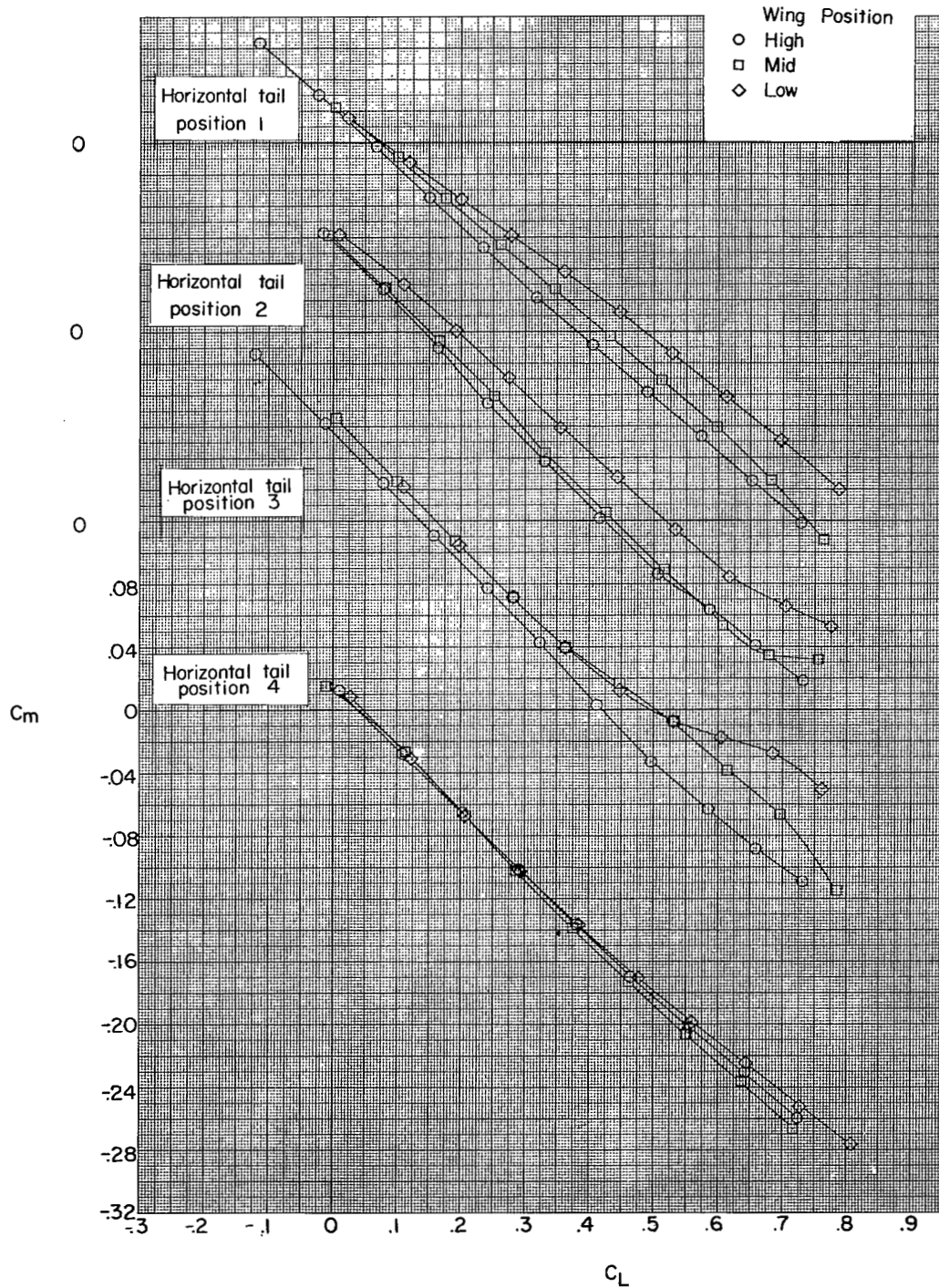
(c) Tail 3.

Figure 6.- Continued.



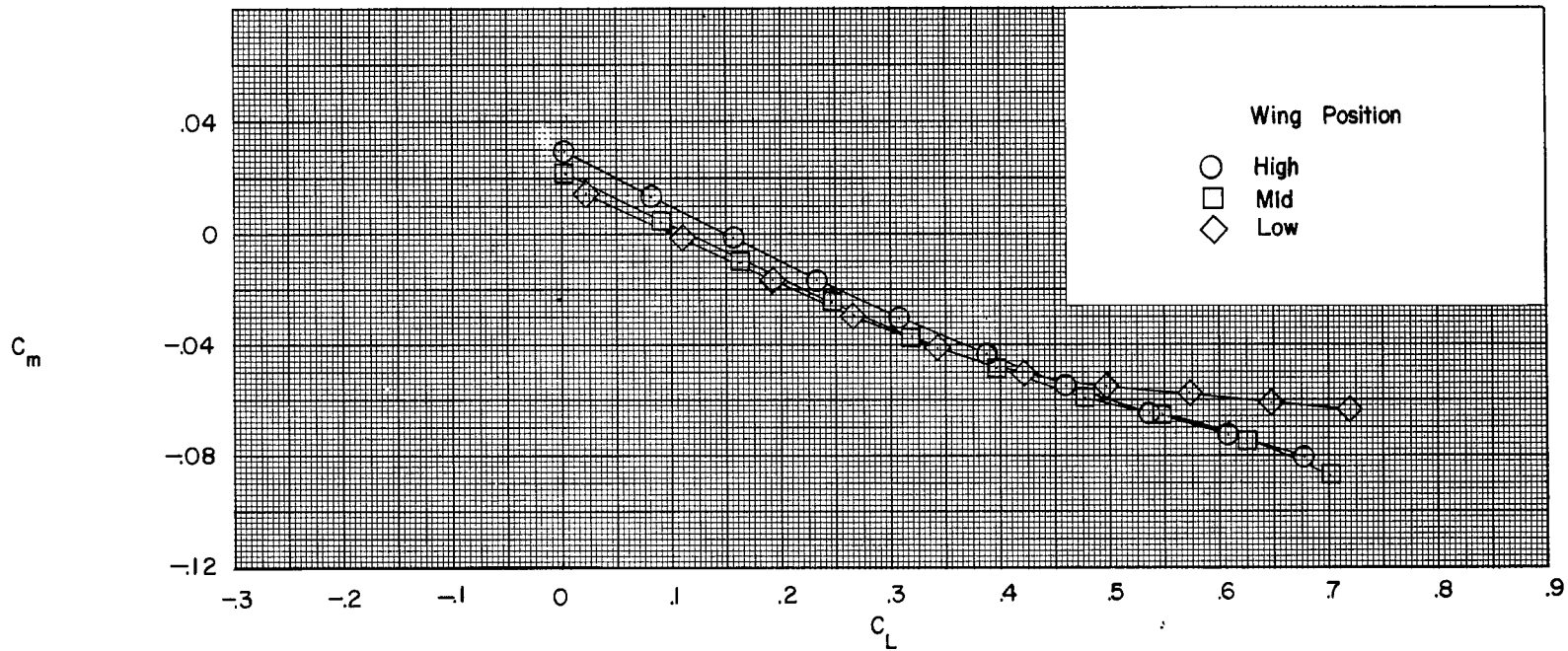
(d) Tail 4.

Figure 6.- Concluded.



(a) Horizontal tail on.

Figure 7.- Effect of wing position on longitudinal stability characteristics for configurations with various horizontal-tail positions.



(b) Horizontal tail off.

Figure 7.- Concluded.

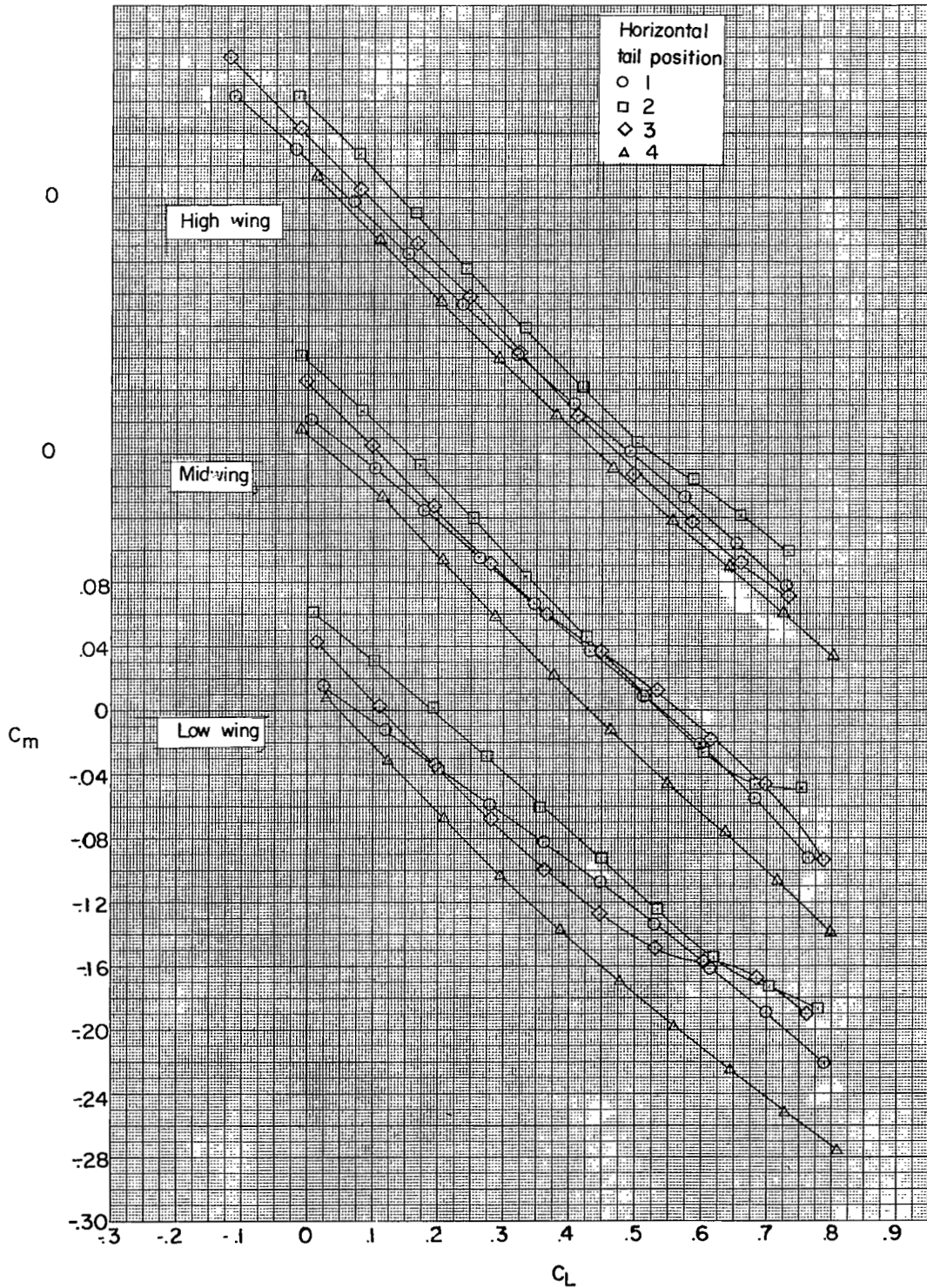


Figure 8.- Effect of horizontal-tail position on longitudinal stability characteristics for configurations with various wing locations.

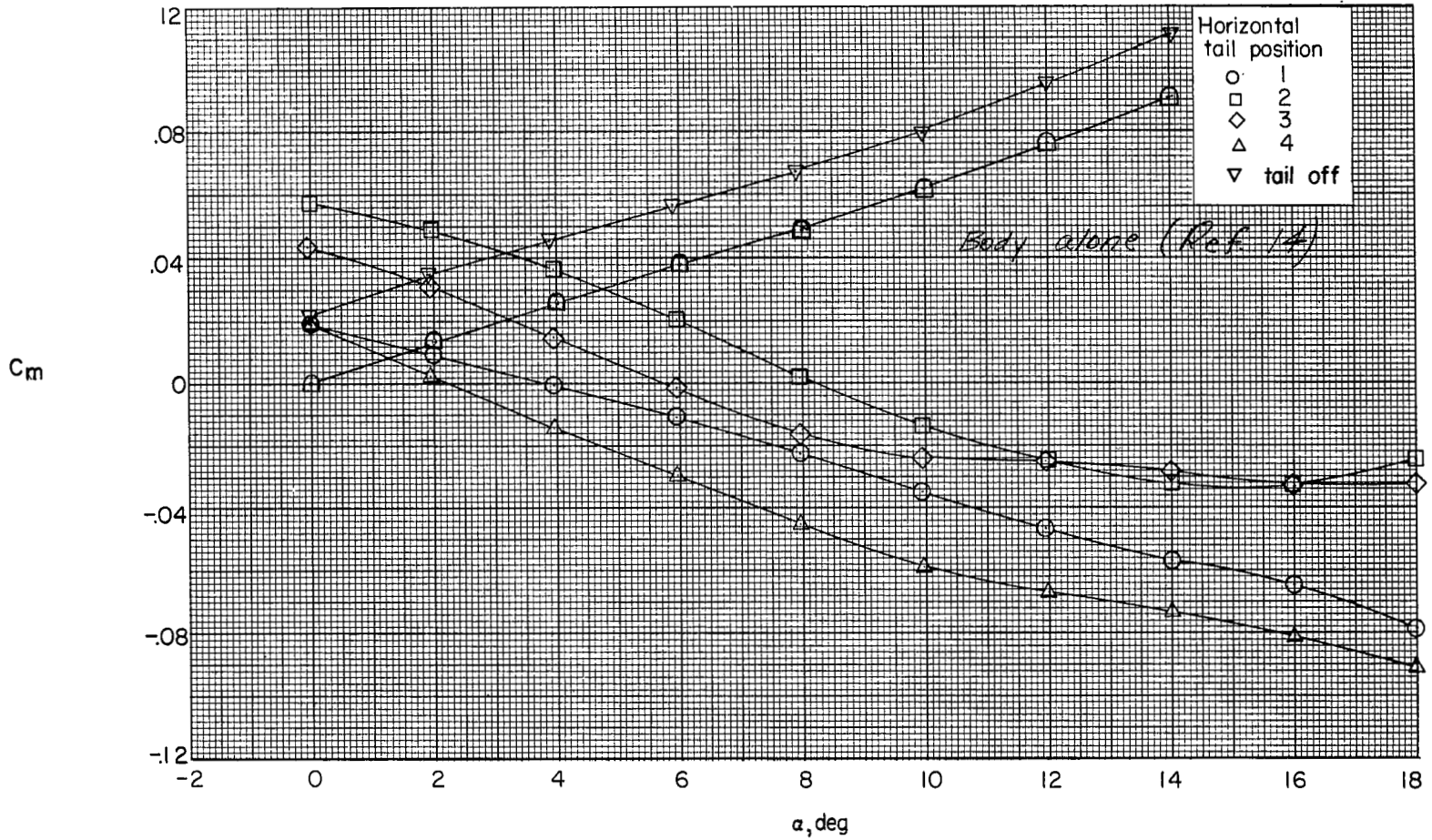


Figure 9.- Effect of horizontal-tail position on longitudinal stability characteristics of the wing-off configuration; $i_t = 0^\circ$.

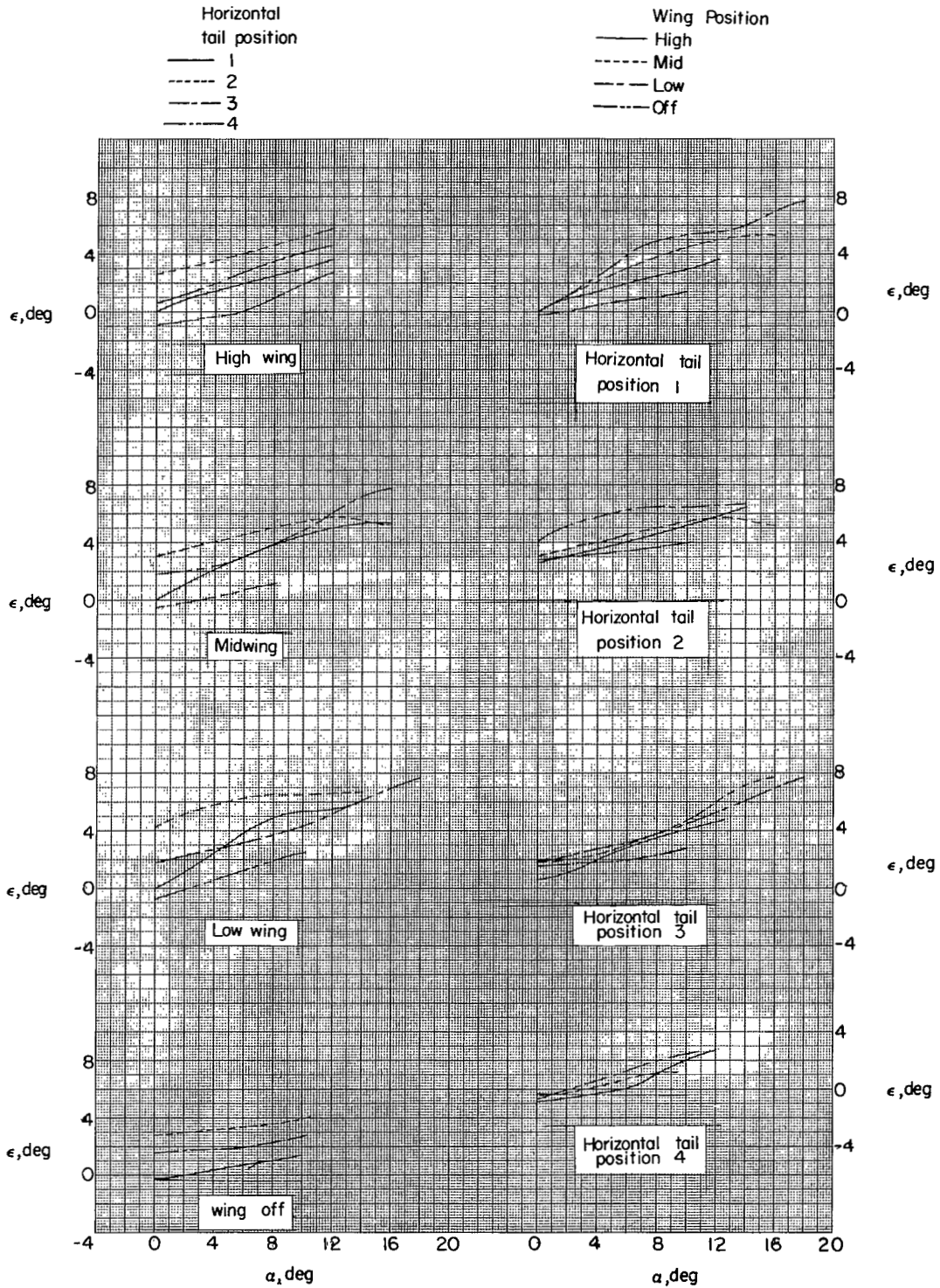


Figure 10.- Effect of wing and tail position on variation of effective downwash angle with angle of attack.

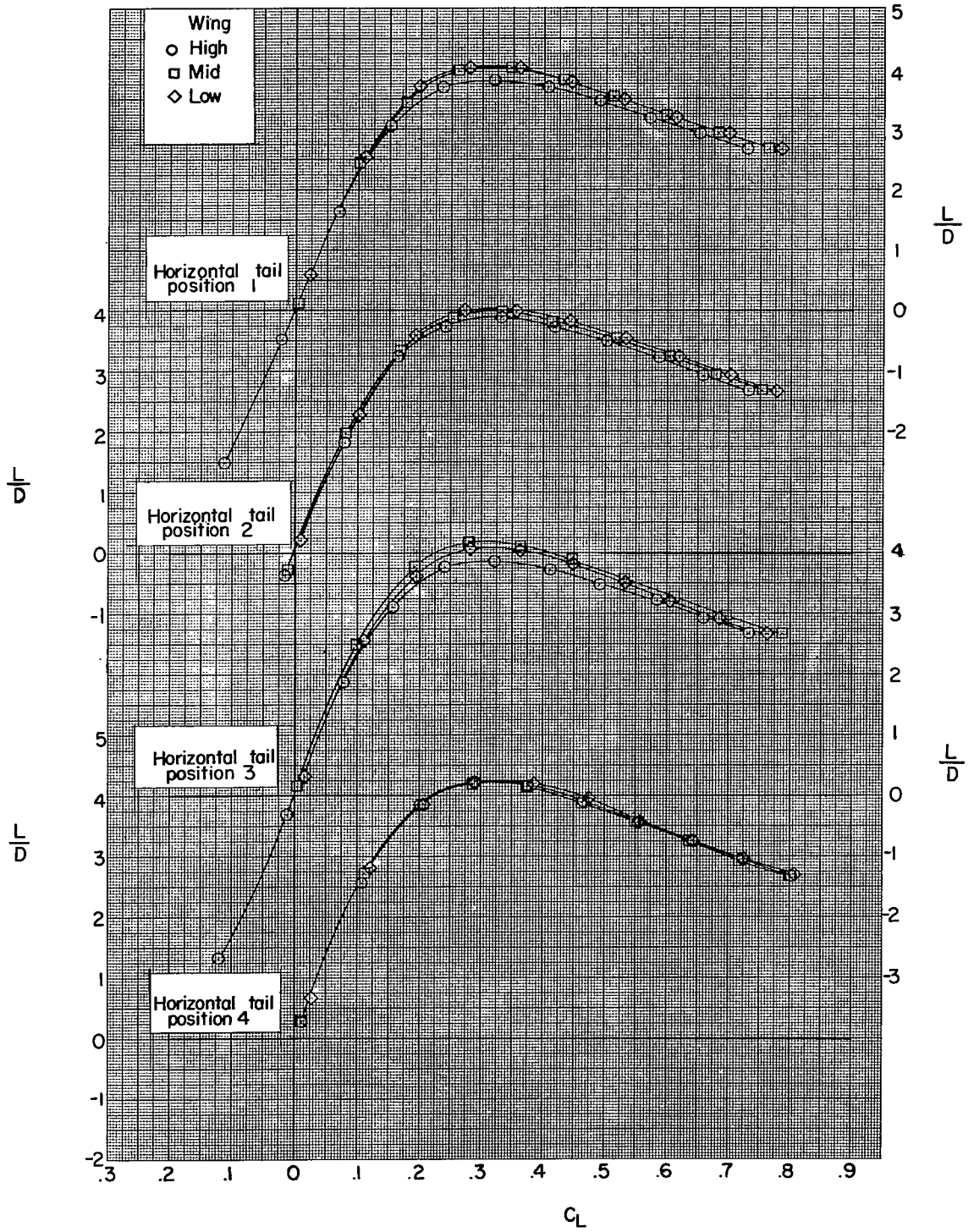


Figure 11.- Effect of wing location on the lift-drag ratio for configurations with various horizontal-tail positions.

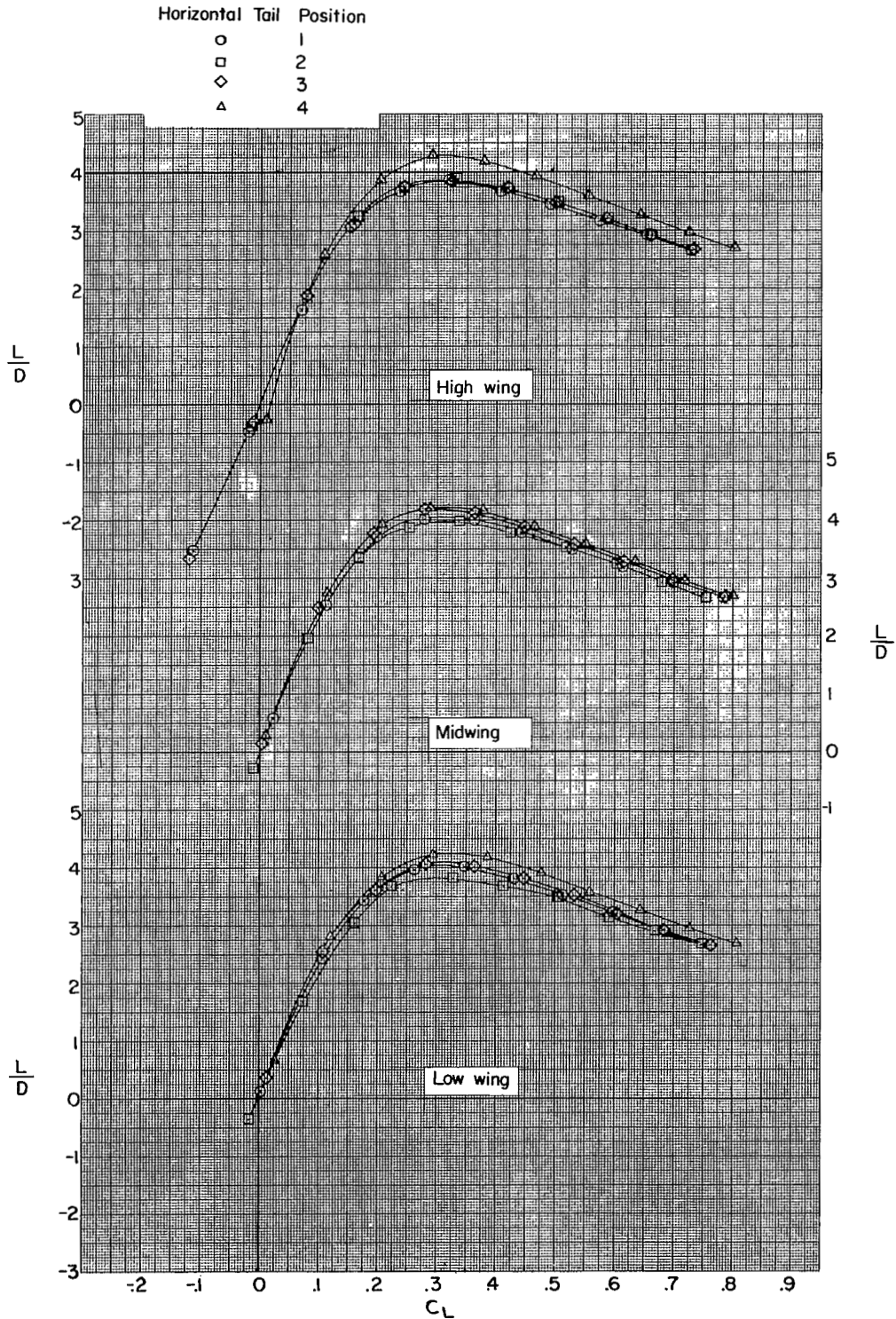


Figure 12.- Effect of horizontal-tail position on lift-drag ratio for configurations with various wing locations.

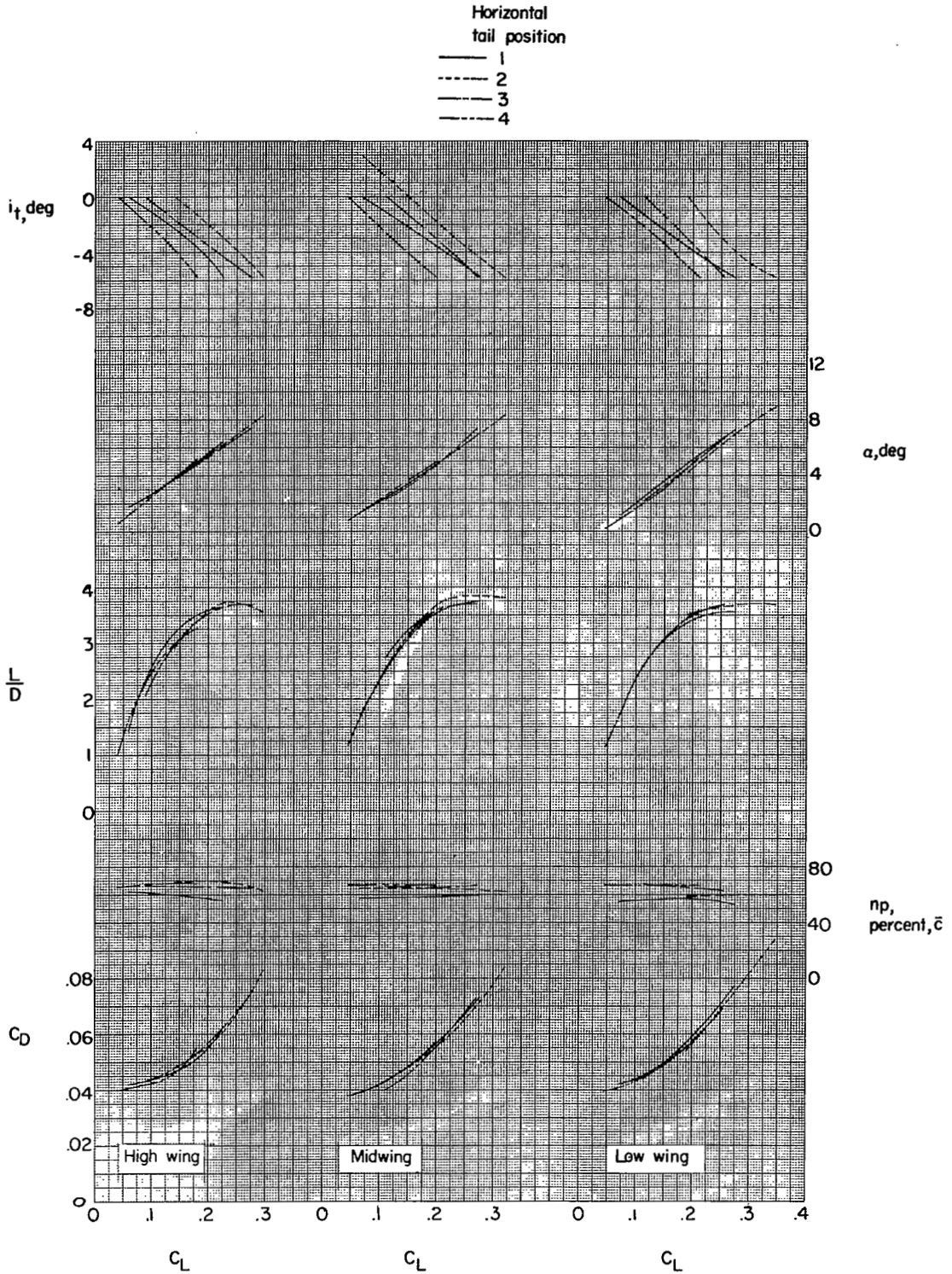


Figure 13.- Summary of longitudinal trim characteristics for various wing and horizontal-tail positions.

NASA Technical Library



3 1176 01437 7817

